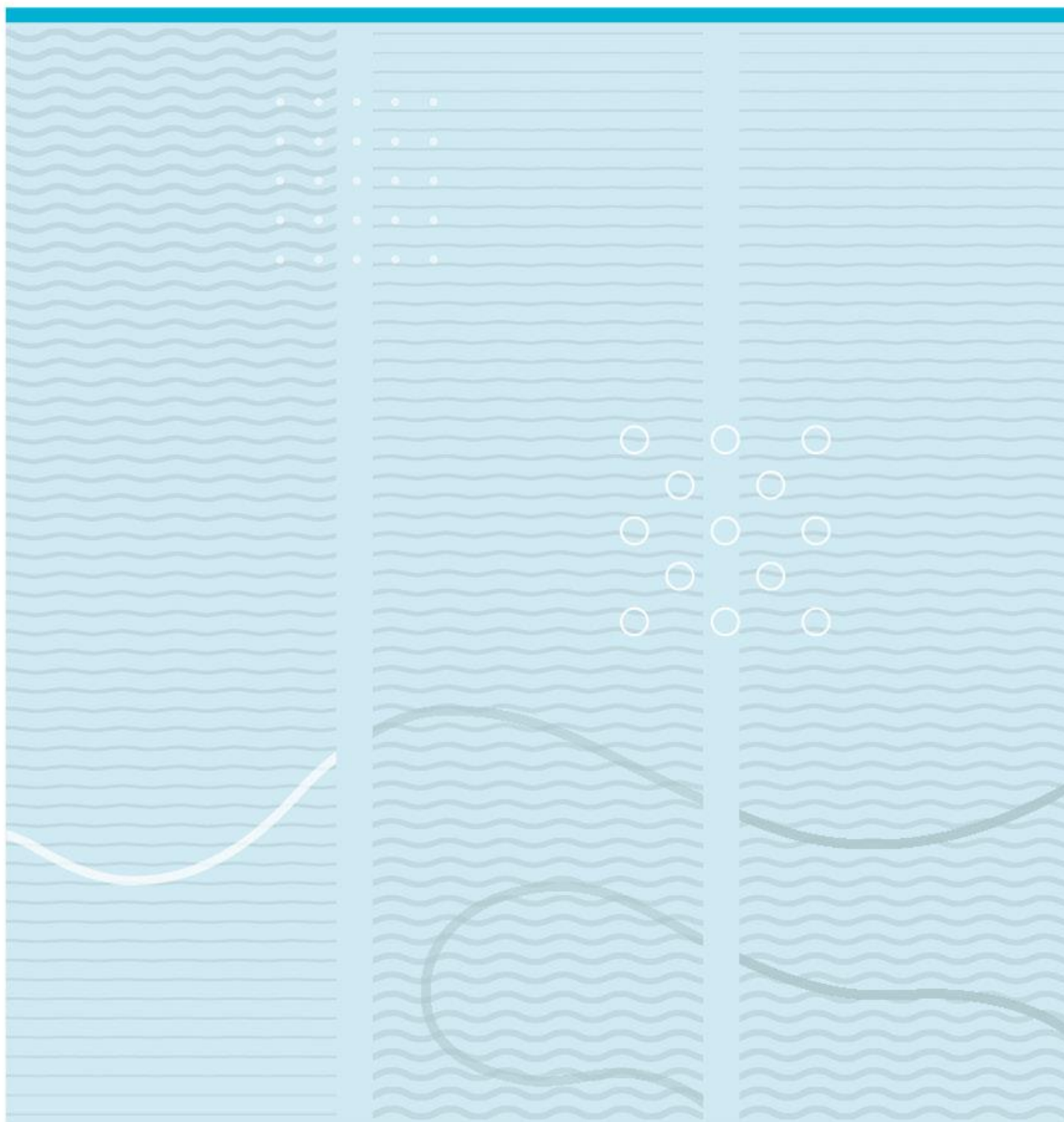


Rashid Ahmed Rifat

Compact Packaging and Testing of Carbon Nanotubes (CNTs) Based Supercapacitors



University of South-Eastern Norway
Faculty of Technology, Natural Sciences and Maritime Sciences
Department of Microsystems
Raveien 215
NO-3184 Borre, Norway
<http://www.usn.no>



© 2023 Rashid Ahmed Rifat

Abstract

This study explored different compact packaging techniques and evaluated their impact on the performance of carbon nanotube (CNT)-based supercapacitors. The increasing demand for high-performance energy storage devices in compact applications has driven the need for efficient packaging and reliable testing methods. Supercapacitors, with their superior power density and long cycle life, hold immense potential for various electronic applications. Various packaging techniques, including coin cell, pouch cell, and chip-type supercapacitor, were employed in this research. Electrochemical characterization techniques such as cyclic voltammetry, impedance spectroscopy, and charge-discharge cycling were implemented to evaluate specific capacitance, power density, energy density, and series resistance. The performance of the supercapacitors was investigated under extreme conditions, including temperatures of -20 °C, 25 °C, and 60 °C. The study thoroughly examined the effects of crimp pressure on coin cell packaging. Additionally, novel design ideas for manufacturing miniature chip-type surface mount supercapacitors are proposed, aiming applications such as memory backup and portable electronic devices. Areal capacitance of 1298 mF/cm² was achieved, which was good compared to its counterparts. Overall, this research highlights the significance of packaging techniques and testing methodologies in enhancing the performance and reliability of CNT-based supercapacitors. The findings contribute to the development of next-generation energy storage systems capable of meeting the increasing demands of diverse industries and applications.

Contents

Foreword	5
List of Abbreviations	6
1 Introduction	8
1.1 Need for Compact Packaging of Supercapacitor	8
1.2 Objectives and Research Motivations	9
1.3 Scopes and Limitations.....	10
1.4 Thesis Outline.....	11
2 Background Studies	13
2.1 Supercapacitors as Energy Storage device	13
2.2 CNT as Electrode Material for Supercapacitors.....	22
2.3 Compact Packaging Techniques for Supercapacitors.....	24
2.4 Performance Evaluation of CNTs based SCs.....	30
3 Experimental Setup & Procedure	37
3.1 Morphology & Material Characterisation of CNTs Electrodes	38
3.2 Packaging and Fabrication of Supercapacitors.....	39
3.3 Electrochemical Characterisation and Testing	44
4 Results and Discussions	49
4.1 Morphology & Analysis of CNTs Electrodes	49
4.2 Effects of Physical & Test Parameters on Supercapacitor Performance	52
4.3 Proposed Chip Type Surface Mount Packaging Solution.....	66
4.4 State-of-the-Art Areal Capacitance with Coin Cell Supercapacitor	70
5 Conclusion and Future Work	76
References	78
List of Figures	85
List of Tables	88
Annexes	89

Foreword

The accomplishment of my joint master's degree in Smart Systems Integrated Solutions (SSIs) at the University of South-Eastern Norway is represented by this thesis. Its completion would not have been possible without the support and guidance of many individuals and institutions.

Firstly, I would like to thank The Almighty for blessing me with the opportunity to pursue a master's degree. I extend my heartfelt thanks to my supervisor, Prof. Xuyuan Chen, and co-supervisor, Dr. -Ing. Raghunandan Ummethala, for their guidance, expertise, and constant support throughout this research journey. Their valuable insights, encouragement, and constructive feedback have been indispensable in shaping this thesis.

I am grateful to Prof. Per Alfred Øhlckers and Mr. Egill Elvestad from nanoCaps for their valuable feedback and never-ending support throughout this industrial thesis from the company. I extend my appreciation to Dr. Pai, Ms. Zekija, Mr. Gaurav, & Mr. Anh Tuan from University of South-Eastern Norway for helping me with the lab facilities & resources.

I would like to appreciate the time and effort from Dr. Ahmad Omar and Dr. Daria Mikhailova from Leibniz Institute for Solid State and Materials Research Dresden, Germany for allowing me work and conduct experiments in such a good research facility.

Appreciation goes to the assistance and collaboration of my fellow researchers and colleagues from USN and nanoCaps who have provided valuable discussions and insights.

I would like to thank my fellow batchmates from SSIs for giving me a good time during the journey and faculty members from all the consortiums for their effort in teaching. European Commission is acknowledged for financing my studies during master's with Erasmus Mundus scholarship. Also, thanks to the Centre for Sustainable Transition at USN for providing me award in the form of a grant for my thesis.

Finally, I would like to express my deepest gratitude to my parents, siblings and friends for their unconditional love, support, and understanding during this challenging endeavour. Their encouragement and belief in my abilities have been a constant source of motivation. With the end of this journey, I hope to continue further in seeking the truth of science through research and innovation.

Vestfold, Norway / July 3rd, 2023

Rashid Ahmed Rifat

List of Abbreviations

Abbreviations	Definition
SC	Supercapacitor
CNT	Carbon Nanotube
AC	Activated Carbon
PC	Pseudocapacitor
EDLC	Electric Double Layer Capacitor
SSA	Specific Surface Area
ACN	Acetonitrile
EDL	Electric Double Layer
ESR	Equivalent Series Resistance
CVD	Chemical Vapor Deposition
APCVD	Atmospheric Pressure Chemical Vapor Deposition
SWCNT	Single-Walled Carbon Nanotube
MWCNT	Multi-Walled Carbon Nanotube
SEM	Scanning Electron Microscope
FE-SEM	Field Emission Scanning Electron Microscope
FTIR	Fourier Transform Infrared
CV	Cyclic Voltammetry
GCD	Galvanostatic Charge Discharge
CCCD	Constant Current Charge Discharge
EIS	Electrochemical Impedance Spectroscopy
WE	Working Electrode
RE	Reference Electrode
CE	Counter Electrode
Al	Aluminium
Ni	Nickel
CNT-SP	Growth of CNTs on Al substrate with <i>Ni sputtering</i>
CNT-DP	Growth of CNTs on Al substrate <i>dip coated</i> with NiSO ₄ solution

CNT-SR	Growth of CNTs on Al substrate <i>spray coated</i> with NiSO ₄ solution
CNT-DR	Growth of CNTs on Al substrate <i>drop-coated</i> with NiSO ₄ solution

1 Introduction

Supercapacitors (SCs) are electrochemical storage devices known for its high-power density and longer lifetime. There are different materials that are used for fabrication of SCs, among them carbon nanotubes (CNTs) as electrode materials show promising potential providing high specific surface area (SSA), good mechanical and electrical properties. Although extensive research has been done on the electrode materials, there has been less light shed onto how these high-potential electrodes can be integrated to a compact device for application specific packaging. High performance electrodes do not necessarily convert to high performance device. While the properties of the material are important for the performance of a SC, compact packaging technique and its optimisation are even more important because growing demand of present-day applications for devices or components like smart biometric card, smart pen, IoT sensor, smart wearables, RFID tag, RAM, etc., for power storage and power backup. As devices for electronic applications are getting miniaturised for portability and usefulness, it is inevitable that a segment of the energy storage systems will also have to follow the same path. Adding to that, for application specific device, both high power and high energy density have been in significant demand in the modern appliances. To that end, compact-packaged SCs based on CNTs can play a vital role in contributing to meet the growing demand in numerous applications in terms of high power as well as high energy density . Moreover, these SCs devices need to be optimised and tested to deliver maximum output to the end user.

1.1 Need for Compact Packaging of Supercapacitor

In SCs critical role is played by the electrodes. Compared to other electrode materials, CNTs have a high SSA, less electrode resistance, high mass loading, binder free method, good mechanical stability and other properties that lead to good performance in terms of specific capacitance, gravimetric capacitance, smaller volume, and less weight of the SC. Whereas, for other types of electrode materials such as activated carbon (AC), they have a complex structure that limits the performance. Among those limitations few notable ones are: its capacitance decreases beyond thickness of few hundreds of micrometres, a binder is needed for the current flow, higher electrode resistance and other properties that limit the potential for a high power and high energy density SC [1]. On the contrary, CNTs do not

have such limitations and are a good candidate for SC application. Also, areal capacitance, which is capacitance per area, for state-of-the-art AC based SCs is as high as 700 mF/cm² [2] whereas the same for CNTs based SCs is found to be more than three times [3]. Nonetheless, good material performance of the electrode does not always convert to good SC, as a device, if the packaging and testing are not optimised. This means proper packaging must be done to ensure that the SC is suitable for the usage in different applications. As the demand for portable electronic devices, smart fingerprint card, electronic wearables, ICs, wireless sensors etc., are exponentially increasing as an energy storage or power backup device, extensive research on compact packaging techniques of SC are inevitable. For such miniature devices, SCs with less area and less volume but high-power, high-energy density, lower resistance and longevity are needed. This is where the compact packaging with CNTs-based SCs come into action. By utilising the superior performance of CNTs electrodes, compact packaged SCs meet the criteria to incorporate into application specific devices having high power, high energy, and faster charging capabilities. Coin cell, pouch cell, and the emerging *chip type* SCs are among the configurations of such compact packages. Compared to larger formats like cylindrical cells, these compact packaging techniques provide numerous advantages into electronics. While there is extensive research on materials properties and conventional cell formats, there is very limited comprehensive study on the compact packaging techniques of SCs. With the growing demand for energy storage applications in electronics more research and innovations in these field is necessary. Having said that, with the potential of high-power delivery and compatibility into ICs and other electronics, emerging energy storage technology such as *chip-type* SCs with CNTs electrodes will be a game changer in the electronics industry. In a survey [4] it was found that compact SCs, for low capacity applications, contribute to more than 45% of the whole SCs market. From the data it is evident that compact type SCs are in need more than ever and they have huge potential in the present and future applications. Therefore, both academic and industrial research on this type of compact SCs are essential to prosper in the field of energy storage technology.

1.2 Objectives and Research Motivations

The primary objective of this thesis is to investigate and explore the compact packaging of SCs as energy storage devices, do the fabrication and testing to evaluate their

performance, with a specific focus on utilizing only CNTs as electrode materials. The motivation behind this research stems from the increasing demand for efficient and high-performance energy storage solutions in various applications of compact and fast-charging devices like smart pens, smart card, sensors, IoT devices, power management for ICs, data backup for SSD-RAM and many more. These devices demand less area and less volume but with high power and fast-charging capabilities. Although there are many research studies on different fields of SCs but there is relatively much less scrutiny on the compact packaging techniques for SCs and its performance evaluation. This study aims to contribute to the understanding and advancement of such SC technology by investigating different compact packaging techniques and evaluating their performance through several electrochemical characterizations and optimisation. Through these investigations, a deeper understanding of SCs can be gained, leading to potential improvements and advancements of SC technology for its integration into rapid charging and compact electronic applications. These optimisations and evaluation will benefit the current energy storage technology field and foster the way towards innovation. Consequently, the thesis aims to investigate these compact packaging techniques at different physical conditions and testing parameters to evaluate their performance and durability, so as to replicate the real-life circumstances. This study also intends to propose a novel design approach for *chip-type* surface mount packaging technology, which is relatively a new topic in the academic research arena, that can contribute to the integration of SCs in compact electronic applications contributing to high-power and fast charging capabilities. Furthermore, this study aims to explore the potential of coin cell SC in terms of areal capacitance, power density, energy density and time constants and compare it with the existing SC technologies. Through this comprehensive research, the study aims to uncover new insights by tapping into several aspects, uncover current limitations, and provide valuable recommendations for future developments in the field of compact SC technology for research and innovation.

1.3 Scopes and Limitations

The scope of this thesis comprises several key aspects related to SCs and their utilization into compact devices. The research primarily focuses on investigating the compact packaging techniques for SCs in terms of coin cell and pouch cell, aiming to enhance their integration into electronic devices by using high performance CNTs as electrode materials.

The impact of different physical conditions and test parameters on the performance of the SCs as well as the evaluation of their electrochemical properties are also studied thoroughly.

However, it is important to note certain limitations within the scope of this research. Firstly, the study primarily focuses on different packaging methods, which may not cover the entire range of packaging techniques for SC applications. Additionally, while the research examines into the evaluation of physical parameters like temperature and pressure effects on SC performance, it may not encompass all possible influencing factors. Moreover, the thesis studied the comparison of the proposed SCs with existing laboratory counterparts. However, it may not cover the entire spectrum of available SC technologies and their variations.

Lastly, although the thesis aims to propose a chip type surface mount packaging solution of SC for electronic applications, it is worth mentioning that this entire field of study is new in the academic research field and near to similar approach is only adopted by only handful of industries. So, the development of a fully functional and commercially viable packaging solution requires further advanced research and development which is beyond the scope of this study.

In this study, it is important to acknowledge the limited resources available in the laboratory for implementing various package configurations and conducting extensive testing. These resource constraints should be taken into consideration when interpreting the results and conclusions presented in this thesis. However, despite these inherent challenges and limitations, the research conducted herein offers significant contributions to the understanding of compact packaging of SCs utilizing CNTs as electrode materials. The findings obtained from this investigation shed light on the potential and obstacles associated with this emerging technology, thereby facilitating the advancement of futuristic energy storage systems.

1.4 Thesis Outline

The thesis begins with an introduction that sets the context for the research, discussing the need for compact packaging of supercapacitors and presenting the objectives, research motivations, scopes, and limitations of the study. The introduction section concludes with

a brief overview of the thesis outline, providing readers with a roadmap of the subsequent chapters.

The background studies chapter delves into the foundational knowledge related to supercapacitors, covering topics such as their role as energy storage devices, the use of carbon nanotubes (CNTs) as electrode materials, various compact packaging techniques, and the evaluation of performance for CNTs-based supercapacitors.

The experimental setup and procedure chapter describes the methods and procedures used in the research. It includes subsections on the morphology and material characterization of CNT electrodes, packaging and fabrication techniques for supercapacitors, and the electrochemical characterization and testing protocols.

The results and discussions chapter presents the outcomes and analyses derived from the research. It encompasses an examination of the morphology and analysis of CNT electrodes, detailed studies on the effects of several physical and test parameters on SC performance, the proposed chip type surface mount packaging solution, and a comparative assessment of state-of-the-art capacitance using coin cell SCs..

The conclusion and future work chapter provides a summary of the key findings and their implications, while also discussing potential directions for future research in the field of compact packaging of supercapacitors.

Following the conclusion, the references section lists all the sources cited in the thesis, ensuring the accuracy and credibility of the research. The list of figures and list of tables provide an index of the visual representations and tabular data included in the thesis, making it convenient for readers to locate specific illustrations. Lastly, the annexes section includes supplementary information, such as raw data, calculations, or additional documentation, which further supports the research conducted in the thesis.

2 Background Studies

The never-ending need for energy has escalated scientific research in batteries, supercapacitors (SCs) and other electrochemical energy storage technology. Sustainable solutions for energy storage have been adapted both by researchers and industry. With the new law approved by European Union to make batteries more sustainable, durable and better performing [5], the choice for sustainable materials is inevitable. Initially, the focus was to develop new technologies and electrode materials for such electrochemical storage devices. Among batteries and other technologies, SCs are of great interest to the scientific community as well industries owing to its high-power density and longer lifetime. Research has been going on different carbon-based electrode materials for SCs such as activated carbon, porous carbon, carbide carbon derivatives, carbonaceous aerogels and xerogels, graphene and their derivatives, and carbon nanotubes (CNTs) [1]. CNTs-based SCs are regarded as high-performance electrode materials for SCs with different low and high voltage applications ranging from vehicles to memory backup in data storage device. These SCs have the great advantage of high-power density and high-energy density. Although there is extensive research on material properties and its implementation, less research studies are available for packaging the SCs, especially the compact packaging and its performance evaluation. Compact packaging techniques like coin cell, pouch cell and chip type SCs have the potential to meet the growing demand for electronic applications where less area and high power are needed.

The literature review chapter aims to provide a comprehensive overview of SCs, encompassing their fundamental properties, electrode materials employed in SCs, compact packaging techniques specific to SCs, the significance of such packaging techniques, as well as the testing and characterization methodologies utilized for evaluating SC performance. This chapter endeavours to present a concise and accessible demonstration of the underlying theory and background relevant to the scope of this study, enabling a clearer comprehension of the subject matter.

2.1 Supercapacitors as Energy Storage device

Supercapacitors, also known as ultracapacitors, are electrochemical devices that has quasi-reversible electrochemical charging and discharging. The general definition was first

defined by B.E.Conway [6]. The type of SCs that has non-Faradaic process and has perfectly electrostatic process as the charge storage mechanism and where the two electrodes are isolated by dielectric is named electric double layer capacitor (EDLC). And the type that involves Faradaic process and in which reversible redox reaction occurs is called pseudocapacitors (PC) [7]. Figure 2-1 shows the classification of EDLC with the electrode materials used for those SCs. EDLCs mainly uses carbonaceous materials due to their porous nature and active surface area. CNTs are promising material for EDLCs owing to its properties and numerous applications. PCs use different types of transition metals and conducting polymers. Hybrid SC use different types of materials in their anode and cathode to make the SC. This study will particularly focus on EDLC type SC based on CNT. Details about the charge storage mechanism, properties of the SCs and their description are discussed later in the report.

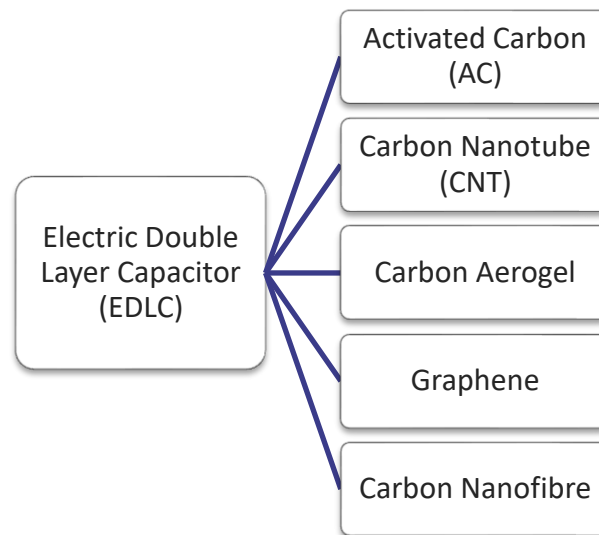


Figure 2-1: Classification of different types of EDLCs and electrode materials used (redrawn from [7])

Gaining insight into the performance characteristics of diverse energy storage devices and establishing their interrelationships in terms of power and energy is of utmost importance. To facilitate such comparisons, the Ragone plot is commonly employed, which allows for the evaluation of energy and power density across a range of energy storage systems. This plot serves as a valuable tool for assessing and contrasting the capabilities of different energy storage technologies. Such a plot of energy - power density is shown in Figure 2-2.

While supercapacitors (SCs) exhibit a notable advantage in terms of high-power density, they are limited in their energy density compared to other energy storage systems. The objective is to simultaneously achieve high energy density and high-power density, enabling a device to store a larger amount of energy and deliver it rapidly when required. This pursuit aims to narrow the gap between traditional batteries and capacitors by reducing it by several orders of magnitude. By bridging this gap, SCs hold the potential to revolutionize energy storage technology, offering a compelling balance between energy storage capacity and rapid energy delivery.

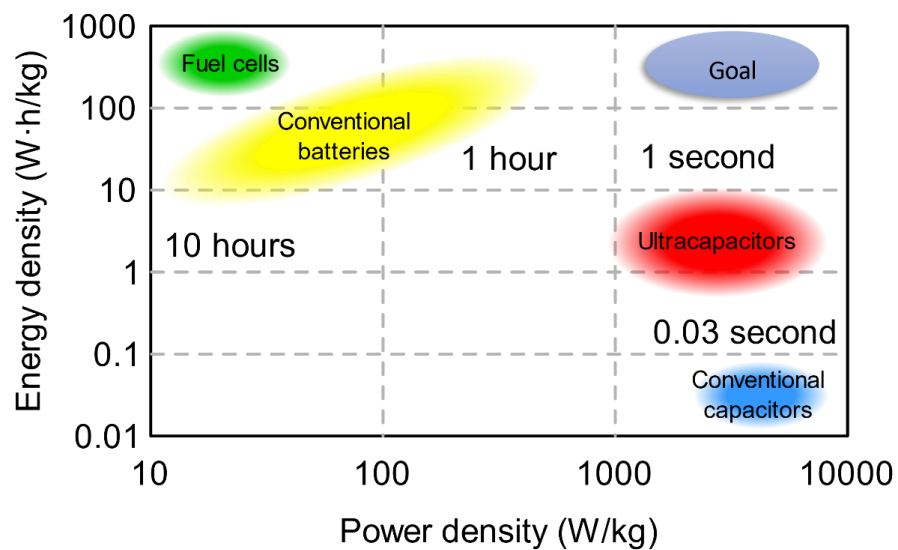


Figure 2-2: Energy-power density represented by Ragone plot for different energy storage systems (adopted and modified from [8])

2.1.1 Constituents of Supercapacitors

There are mainly four essential parts of a SC. A) Electrode B) Electrolyte C) Separator D) Current Collector. Each of the part is discussed in the following section.

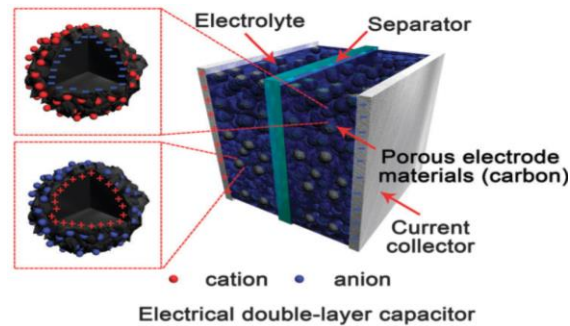


Figure 2-3: Schematic of EDLC showing its components [9]

A schematic of an EDLC with the four main components can be seen in Figure 2-3.

Brief discussion about each of the components of SC are given below-

- A. **Electrode:** Material selection for the electrodes is essential for the performance of the SCs. The properties of the electrode materials should have high specific surface area (SSA), high electrical conductivity, chemical and thermal stability, low-cost and environment friendly [7], [10]. EDLC type behaviour can be seen in carbonaceous electrodes. These electrodes do not involve Faradaic process and can store charge at the surface of the electrodes. Carbonaceous materials consist of a wide from graphene to nanofibers and nanotubes. CNT plays an important role in reaching high capacitance owing to its many useful properties like high SSA, high electrochemical stability and high mechanical properties and many more [11]. More details about CNT materials and their roles in SCs will be discussed in the next sections.
- B. **Electrolyte:** The electrolyte serves as a crucial component in dictating the performance characteristics of supercapacitors (SCs). The physical and chemical properties of the electrolyte play a vital role in determining the overall efficiency and effectiveness of the SC. The selection and optimization of the electrolyte can significantly impact important parameters such as the working potential window, capacitance, cycle life, and energy-power density of the SC. By carefully tailoring the electrolyte composition, it becomes possible to enhance the operational range, maximize capacitance, prolong the cycle life, and achieve optimal energy and power densities for the SC .

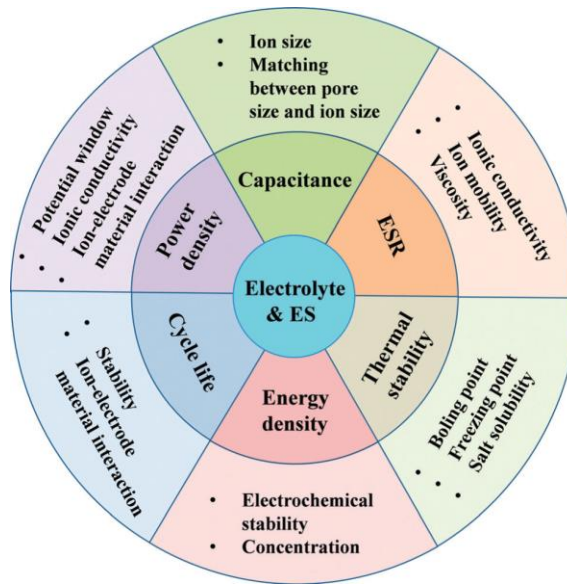


Figure 2-4: Effects of different electrolyte on SC performance [adopted from [9]]

Figure 2-4 shows the most important properties of electrolytes affecting the performance of SC. Among many developments of SC, to increase the working potential window, i.e., increasing the voltage of the cell, is of great interest. It is because if the working potential is increased it can essentially increase the energy density of SC as can be seen from Eq. 1.

$$E = \frac{1}{2} CV^2 \quad (1)$$

Here, E is the energy density of the cell, C is the capacitance in $F g^{-1}$ and V is the cell voltage. The energy density of supercapacitors is directly proportional to the square of the cell voltage, indicating that increasing the voltage is a more efficient approach for enhancing energy density compared to increasing electrode capacitance. Therefore, the development of electrolytes with a wider potential window is crucial to enable higher voltage operation and maximize energy density. By focusing on expanding the potential window of the electrolyte, significant advancements can be achieved in enhancing the energy storage capabilities of supercapacitors. There are many types of electrolytes as liquid, solid state or quasi solid state or ionic electrolyte that were reported in the literature.

There are many factors in the nature of the electrolyte that all have influence on the EDLC capacitance and performance, that includes a) type of the ion; b) size of the ion; c) concentration of ion; d) ion-solvent interaction; e) electrolyte-electrode

interaction; and f) working potential window [9]. Moreover, the electrolytes must be in operating condition within -30°C to $+70^{\circ}\text{C}$ temperature.

Aqueous electrolytes have less electric double layer (EDL) thickness than non-aqueous electrolytes. So, the total capacitance is greater in the aqueous electrolyte than that of the non-aqueous one. But the main disadvantage of the aqueous is the low discharge voltage along with high corrosivity and short temperature range. On the contrary, organic electrolytes, which falls under non-aqueous electrolytes, have a larger operating voltage ($>2.3\text{ V}$) and good stability in a wide range of temperature [1]. But there are issues with organic electrolyte such as higher cost, lower conductivity and lower specific capacitance that must be taken into consideration. Using organic electrolyte, a study showed that the capacitance of EDL SCs increases with the decrease of the ion size [12]. Dimethylpyrrolidinium tetrafluoroborate dissolved in Acetonitrile (DMP- BF_4/ACN) is such an organic electrolyte with small cation, higher potential window and greater stability.

C. **Separator:** In the construction of a SC, a separator is necessary to create a physical barrier that separates the two electrodes and prevents short circuits. The primary function of the separator is to facilitate the efficient transport of ions without undertaking any chemical reactions. The ideal porosity of the separator should be optimized to ensure an adequate supply of electrolyte to the SC. The separator material should have small and uniform pore sizes to prevent short circuits resulting from electrode particle migration or dendritic growth [13]. Electrolyte retention is another role of the separator. By retention of the electrolyte, separators prevent leakage or excessive evaporation, maintaining the stability and durability of the SC. Separators also provide with mechanical support SC cell to maintain the structural integrity during operation and preventing damage or deformation to the cell. Typical separator materials used in SCs consist of glass fibre, cellulose, ceramic fibres, or polymeric films [7]. Figure 2-5 shows a separator used to separate the carbon electrodes for a cylindrical SC.

Glass fibre separators provide rapid filtration while maintaining excellent particle retention capabilities. The separators used in SCs are constructed from borosilicate glass fibres, providing them with exceptional resistance to various organic and

inorganic solvents. These separators exhibit thickness variations ranging from 0.3 mm to 1.0 mm and possess the capability to withstand high temperatures up to 500 °C. [14].

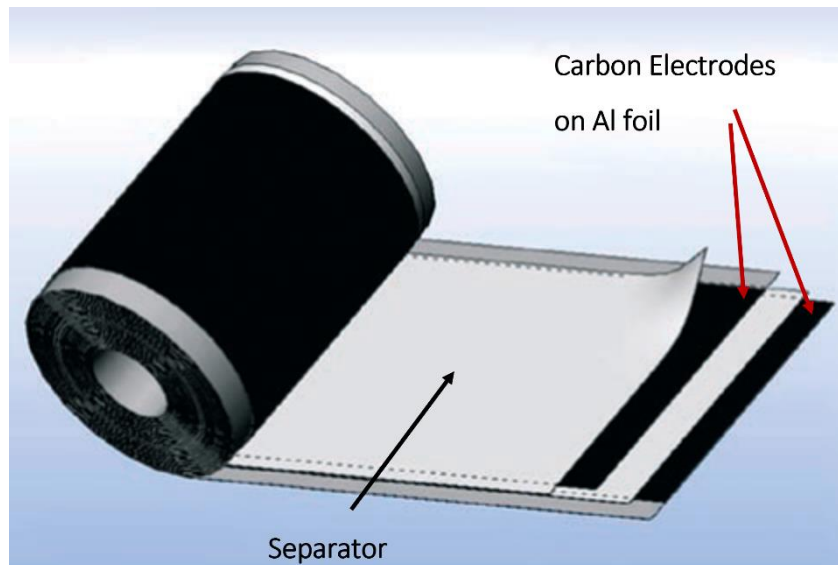


Figure 2-5: Carbon electrodes on Al foil (current collector) and separator used in EDLC
[15]

D. **Current Collector:** The current collector facilitates efficient charge transfer via the external load or circuit. Electrons are collected from the electrode and supplied to the output device. To ensure optimal performance of the SC, the current collector must have superior conductivity (electrical). Its primary function is to minimize contact resistance, allowing for smooth electron flow. Therefore, for the enhancement of the performance of the SC few aspects of the current collector are essential such as: high electrical conductivity, lower contact resistance, high electrochemical stability, flexible and light in mass [16]. In general, current materials such as aluminium, iron, and steel alloys are commonly used as current collector. To ensure that the contact resistance is reduced, the activated materials is coated, or grown chemically on the current collector. Typically, aluminium foil is chosen as the current collector due to its ability to efficiently carry high currents, its chemical stability, and its relatively low cost [17].

2.1.2 Brief Discussion of EDLC Mechanism

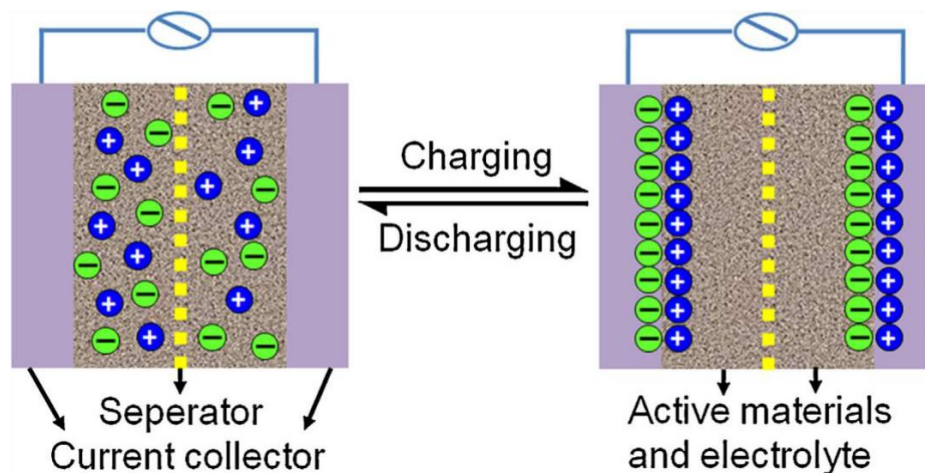


Figure 2-6: Schematic of charge and discharging mechanism in EDLC [18]

Now that the basic parts of SC are known, the mechanism of SC can be described in a proper manner. As mentioned previously, there are generally two mechanisms of charge storage for SCs:

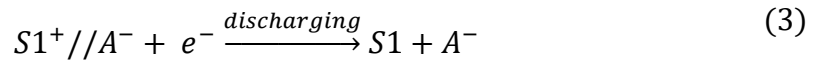
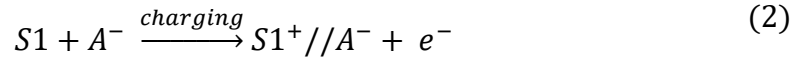
1. EDLC: The charges are stored electrostatically as electric double layer capacitance at the interface of the electrode of the SC and
2. Pseudocapacitance: Storing the charges in faradaic mechanism at the interface of the electrode material [6].

EDLCs operate based on a capacitive mechanism, where electrostatic forces play a significant role. Capacitance is generated at the plane where the electrolyte and electrode come in contact due to the electrode-potential-dependent accumulation of electrostatic charges. The charge is stored electrostatically the electrolyte ions are adsorbed onto the surface of the active material. There is a lack of electric charges on the surface of the electrode due to the accumulation of charge. Meanwhile, to maintain a neutral electron balance the electrolyte compensates by accumulation of charge-carrying ions [7], [15], [17].

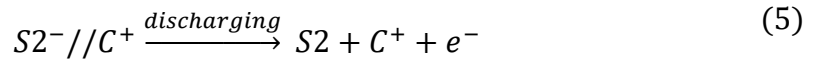
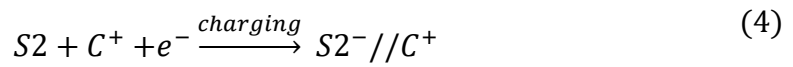
The charge-discharge process of the EDLC can be mathematically described using the subsequent expressions. S_1 and S_2 are electrode surfaces, anions are denoted as A^- , cations as C^+ , and the electrode-electrolyte interface is indicated by the " //" symbol. These equations provide a quantitative representation of the electrochemical reactions

happening during the charge-discharge cycles of the EDLC. So, the equations can be expressed as Eq. (2)–(7) [17].

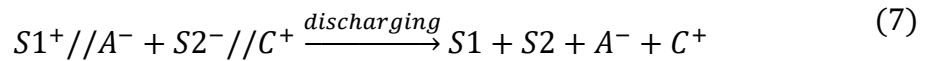
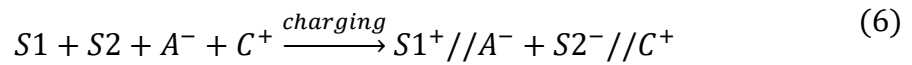
For the positive electrode:



For the negative electrode:



So, the overall charging and discharging shown in Eq. (6) and (7) becomes:



Several theories and models are used for explaining the formation of EDLC are based on widely known model theories of Helmholtz, Stern and Gouy-Chapman [19].

In the context of the pseudocapacitance electrode for PC, electrochemical reactions occur in two distinct manners. Firstly, there is a process of charge transfer that is Faradaic. Secondly, there is a redox reaction that takes place either at the surface of electrode or in close proximity to it. As a potential is applied on the electrode material, it experiences fast and highly reversible redox reactions. This causes the rise of pseudocapacitance due to the alteration in the valency number of the electrode material, thus leading to the transfer of electrons. Figure 2-7 shows schematic of a PC showing its components.

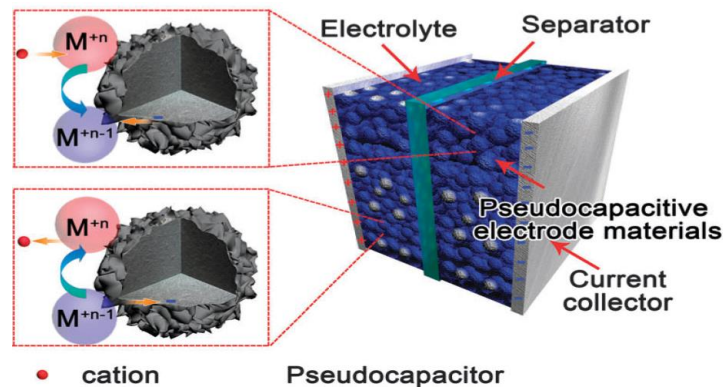


Figure 2-7: Schematic of a PC showing its components [9]

2.2 CNT as Electrode Material for Supercapacitors

The selection of materials for SC plays a crucial role on its performance, as noted earlier. The main aspect to fulfill the requirement of high capacitance is using high SSA electrodes. Carbonaceous materials are widely used for its high SSA, and relatively low cost. Among different carbonaceous materials, carbon nanotubes (CNT) are regarded as promising electrode materials for SCs because of their high SSA, high electrical conductivity, excellent electrochemical stability and good mechanical properties, among other advantages. Eq. (8) shows that the surface area (A) affects the electric-double-layer-capacitance directly. In the case of CNT, this area corresponds to the active surface of the porous CNT electrode.

$$C \propto \frac{A}{d} \quad (8)$$

This means that with high SSA of CNT electrodes the capacitance will also be high.

Figure 2-8 shows the graphical representation of SWCNT and MWCNT.

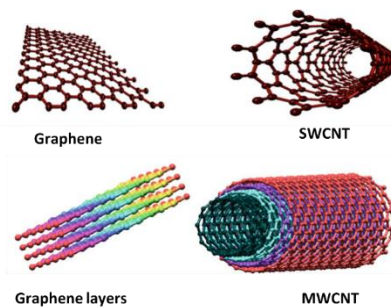


Figure 2-8: Diagram of SWCNT and MWCNT formed by rolling graphene sheets [11]

One of the most commonly used methods for the synthesis of high quality CNTs is by chemical vapor deposition (CVD). CVD for synthesizing CNTs involves preparing a catalyst-

coated substrate (for e.g Ni catalyst on Al foil), introducing a carbon feedstock gas into a heated chamber, and allowing the carbon atoms to accumulate and form nanotubes on the catalyst surface. The growth process is controlled by adjusting parameters such as temperature, gas composition, and flow rate, and the resulting nanotubes are collected after cooling down the chamber [11]. Both SWCNT and MWCNT can be synthesised using the CVD method [20], [21].

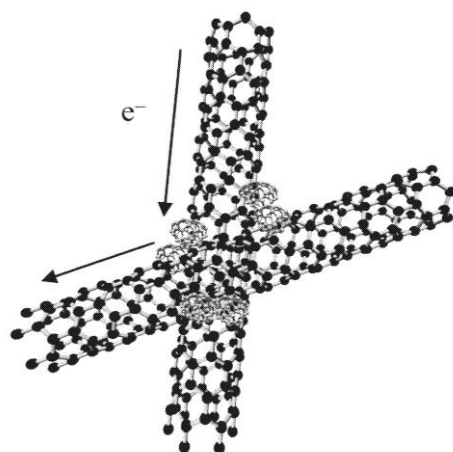


Figure 2-9: Illustration of chemically interconnected cross-linked CNT [22]

There are many useful properties of CNTs that help to boost the functioning of CNT based SCs. Within the CNT network the ions of the electrolyte can diffuse through easily and at a faster rate which results in lower ESR for the electrode [23]. Lower ESR means that the charging time of the SC device will be faster. A recent study showed a promising technique to directly grow MWCNTs on aluminum foil, specifically for use as SC electrodes [24]. The results exhibited good specific capacitance and cyclability in charge-discharge process. Researchers from University of South-Eastern Norway have developed a similar technique by CVD method to synthesise interconnected cross-linked CNT on Al foil using atmospheric pressure chemical vapor deposition (APCVD) that resulted in achieving high areal capacitance of approximately 2 F/cm² [25]. The APCVD process uses different gas compositions for the growth of the CNTs.

Figure 2-9 shows an illustration of chemically interconnected cross-linked CNTs that enhances the mechanical features, higher tensile strength of CNTs, high surface area and greater porosity that is useful for SC application [26], [27]. So, this technology of growing CNT allows to achieve remarkable properties, such as a significantly high surface-area-to-

volume ratio, rapid ion diffusion dynamics and excellent electron conductivity, leading to an extraordinary specific capacitance with an organic electrolyte. Additionally, the technology exhibited an impressively low series resistance of less than 100m Ohm/cm² at 1kHz [25], [28].

2.3 Compact Packaging Techniques for Supercapacitors

The packaging of SCs play a crucial role in their overall performance, reliability, and integration into a wide range of applications like mobile and wearable electronics, power backup systems, IC power management, transportation and vehicles, defence and aviation sector, and more [29]. Moreover, compact packaging techniques are particularly important for achieving efficient space utilization, enhancing power density, and enabling the miniaturization of energy storage systems. When it comes to compact packaging of SC, usually on a laboratory and scale and for research purpose coin cell, pouch cell, cylindrical and swagelok type cells are usually tested and validated by the research community. There is much academic research most based on materials of SCs that have been done for demonstrating the performance of CNT based SC for different application [30]–[33]. One study report about the assembly and packaging of several SC cells into a module [34] that demonstrated energy density performance of the SC module. Another research study by Brahim et al [35] demonstrated high volumetric capacitance and other testing performances with cylindrical and pouch cell formation.

Unfortunately, there is less comprehensive study based on the packaging of compact SCs. Research has been going on also with other types of SCs like micro supercapacitors (MSCs) for small and portable electronic applications. Few research studies report about on-chip SC and are suitable for electronic equipments such as implantable medical devices, MEMS device and flexible electronics [36]–[39]. These research demonstrations provide insights into the challenges and advancements in prototyping, miniaturization, on-chip integration, and fabrication methods of SCs. They explore different approaches to improve performance, energy density, and power density of SCs for various applications. Compact packaging techniques are also adopted by many commercial industries owing to its numerous small device applications as battery assist, power backup and power storage device [40], [41]. Commercial SCs comes in a range of form factors that includes coin, pouch, cylindrical and prismatic types. SCs are commercially manufactured to meet the

growing demand of small and portable electronic applications. Interestingly, there is an emerging SC type that is much smaller and has higher power capability. These chip like SCs have to potential to contribute to the energy storage systems. The next sub-sections will discuss about few compact packaging techniques for SC application that are of relevant for this study.

2.3.1 Coin Cell

Coin cell, also called button cell, are used in small electronic devices. In laboratory scale, performance of a SC is usually tested and validated with coin cell setup on. In the case for SC, two electrodes are typically used, which are separated by a porous membrane. High-surface-area materials are used as electrodes, such as CNT, that can store and release electrical charge efficiently as discussed in 2.2. The porous membrane serves as a separator, allowing ions to move between the electrodes while preventing electrical short circuits. For the coin cell parts there are two metal casings on the top and bottom, a conical spring, and a spacer (metal disk). These parts are made out of stainless steel¹ and the top cap has a sealing gasket inside made of polypropylene [42]. To ensure hermetic sealing of the SC cell, the assembly of the coin cell needs a pressure (known as crimp pressure) that is applied on the top casing shown in Figure 2-10. The spacer and the spring are used for the mechanical stability and to ensure proper connection of the electrodes with the top and bottom cases. More details about the assemble and packaging will be discussed in Experimental Setup & Procedure section.

¹ Grade type SS304 contains up to 18% Chromium and up to 8% Nickel.

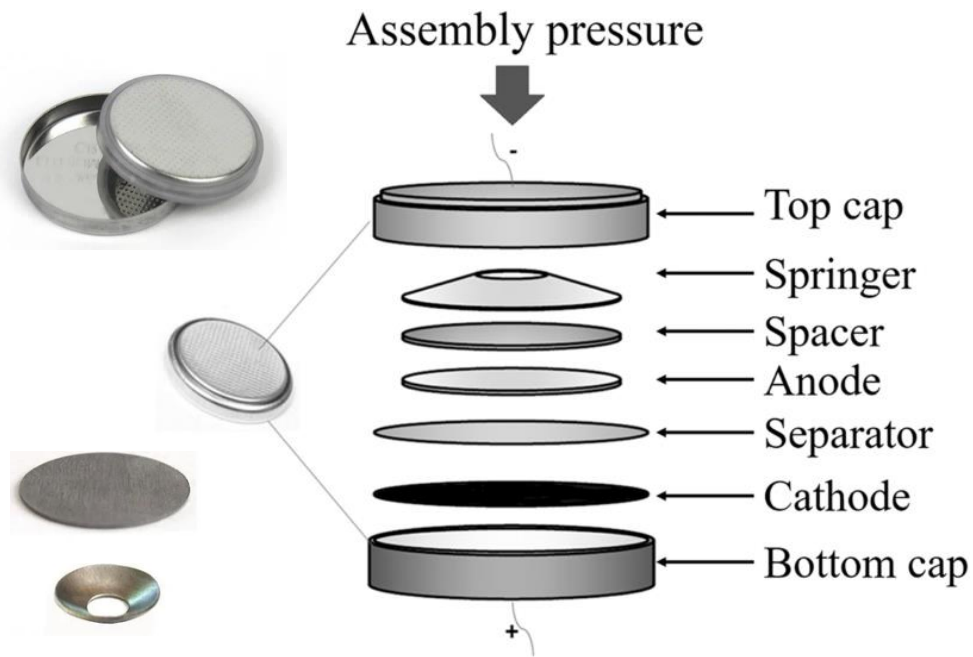


Figure 2-10: Schematic of coin cell parts and configuration [42]

The size of the coin cells usually has a distinct code number that represents the diameter and thickness of the casing. More generally the code starts with a CR that means coin cell (C) and round shape (R). For the numeric part, the first two digits mean the diameter of the cell in mm and the last two digits mean the thickness or height of the cell in tenths of a millimetre. For e.g., for coin cell model CR2032 the diameter is 20 mm, and the height is 3.2 mm.

Coin cell SCs have several advantages. They have a compact size, making them suitable for applications where space is limited. They can be easily integrated into small electronic devices or used as standalone energy storage units. Coin cell SCs exhibit exceptional characteristics, including high power density and extended cycle life. These attributes allow for rapid charge and discharge cycles to be sustained over an extended period. The high power density of coin cell SCs enables them to deliver and store energy efficiently, making them suitable for applications that require rapid energy release. Additionally, their long cycle life ensures that the SCs can endure multiple charge and discharge cycles without significant degradation, providing prolonged usage and reliability in various applications. [43]. These SCs provide quick bursts of power, which is beneficial in scenarios where high-power requirements are necessary, such as in wireless sensors, medical devices, or backup power systems.

2.3.2 Pouch Cell

Pouch cell design has gained considerable attention in both research and industry as a viable option for SCs. Pouch cells are part of surface mount device (SMD) technology that enables attaching these devices directly onto a circuit or PCB. This design involves arranging electrode sheets and separators in layers inside a polymer bag. One of the key advantages of pouch cells is their flexibility in design, allowing for the stacking of any desired number of electrodes in various shapes. As long as the soldered current collector tabs are properly connected to the appropriate terminals within the cell, this design offers significant design freedom [44]. The polymer bag used in the assembly of these components offers flexibility to allow volume expansions, allowing for a high degree of customization in cell capacity without significant difficulties [45]. Moreover, the pouch cell design optimizes space utilization, achieving packaging efficiency of up to 90-95%, which is the highest compared to other packaging designs [44]. Devices utilizing pouch cells tend to be thinner, demonstrate lower ESR value, and achieve higher energy and power densities [44].

Pouch cells mainly have six parts: a) Polymer bag ; b) metal tabs ; c) heat sealant ; d) electrodes ; e) separator and f) electrolyte. The polymer bag acts as the outer package of the cell generally made of polymer or aluminium laminated with polymer. The metal tabs act as the positive and negative terminal of the cell and are needed to make electrical connections outside the pouch cells. The tabs are made of aluminum or nickel and have a heat sealant on them made of thermoplastic bonding film that ensure that these tabs stay in position and make proper sealing with the pouch bag under high temperature sealing. A separator is placed between the two electrodes (anode and cathode) similar to coin cell. Finally, the electrolyte is put onto the separator inside a N₂/Ar filled glovebox (to ensure moisture free environment). Figure 2-11 shows a schematic of a pouch cell configuration.

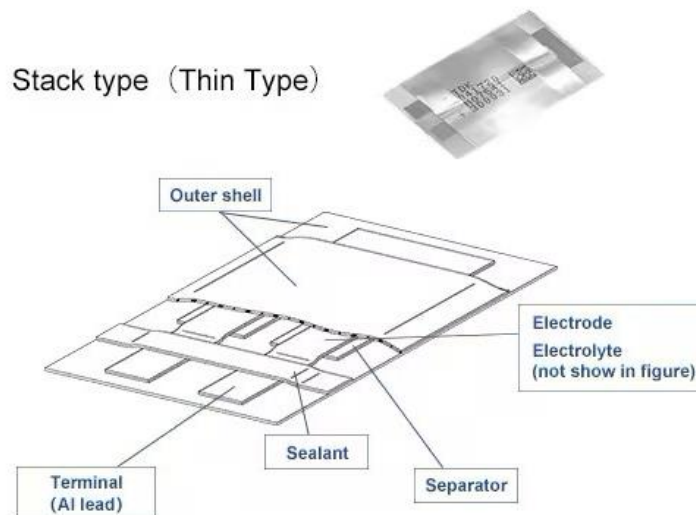


Figure 2-11: Schematic of a pouch cell configuration [41]

Although there are several advantages of pouch cell, its rigidity depends on how well the cell is constructed. They may be more sensitive to mechanical damage due to their flexible nature, requiring careful handling and protection. Pouch cells can also have slightly lower mechanical stability compared to rigid formats, which may affect their long-term durability and cycling performance. But these are mostly true in a laboratory setup. Industrially made pouch cells tend to be more rigid and durable. There are many applications of pouch cells, especially in compact devices or systems. Among them smart biometric card is a promising technology that uses very small pouch cells for powering the device. This means that these compact SCs need to have much less area but also high power for rapid charge delivery.

2.3.3 Chip Type EDLC

Among the types of SCs form factor, chip-type SCs are relatively less footprint both in the research and industrial arena. These chip like structured SCs, are perfectly compatible for devices that have numerous application. To meet the consumer demand for smaller and thinner electronic components in portable devices, there are industries that pioneered the commercial manufacturing of chip-type EDLC for SC application. One such company is Seiko Instruments Inc. (SII) from Japan that introduced a new type of chip-type EDLC and claims to be the world's thinnest and smallest chip-type EDLC, designed for small portable devices like smart pen, smart card, memory backup, ICs etc. These compact packaged EDLCs are

surface mount device that have various applications where compact design is intended. As per Seiko, the chip-type rectangular shaped EDLCs increase volumetric efficiency by 50% and reduces mounting height by 20%. They use activated carbon and organic solvent in its electrode and electrolyte, respectively, the chip-type design and superior air-tight ceramic package ensure improved leakage current and long-term reliability. With a size of 3.2 mm in length, 2.5 mm in width and thickness of 0.9 mm (shown in Figure 2-12), this SC has high capacitance (14mF), quick charge characteristics, and reflowable Pb-Free design, these EDLCs are suitable for backup memory for CPU or DRAM, clock functions, and power management in various portable electronic device and wireless sensor networks.

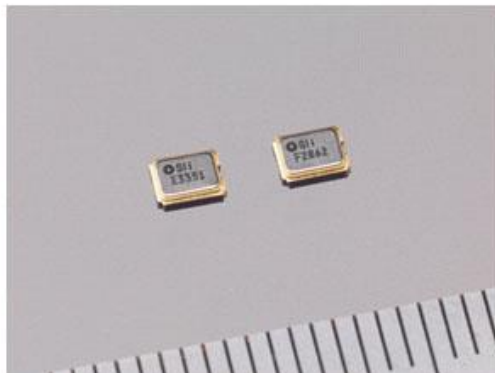


Figure 2-12: Chip-type EDLC from Seiko Instruments Inc. [40]

Seiko's chip-type EDLC offers smaller and thinner capacitors with improved performance and reliability. These EDLCs cater to the demand for compact electronic components in portable devices and can be used for various applications such as backup for memory, power management, and energy harvesting to open new research opportunities in the field of energy storage technology[40]. The literature on the assembly and packaging of chip-type EDLCs is currently quite limited. However, there is a growing interest within the research community to explore and investigate this design for testing and validation purposes. These SC have the potential to greatly impact the energy demand in the electronic industry. The author of this study was motivated to conduct research on the potential design solutions for chip-type EDLCs. The aim was to address the existing knowledge gap and contribute to the understanding and advancement of this particular area of EDLC SC technology. Further discussion about this chip-type SC will be mentioned later.

2.4 Performance Evaluation of CNTs based Supercapacitors

SCs have to be evaluated based on many performance metrics and factors that involves type of electrode material, electrode thickness, electrolyte, current collector, mass loading of the active material, cell configuration, testing methods, testing parameters and many more.

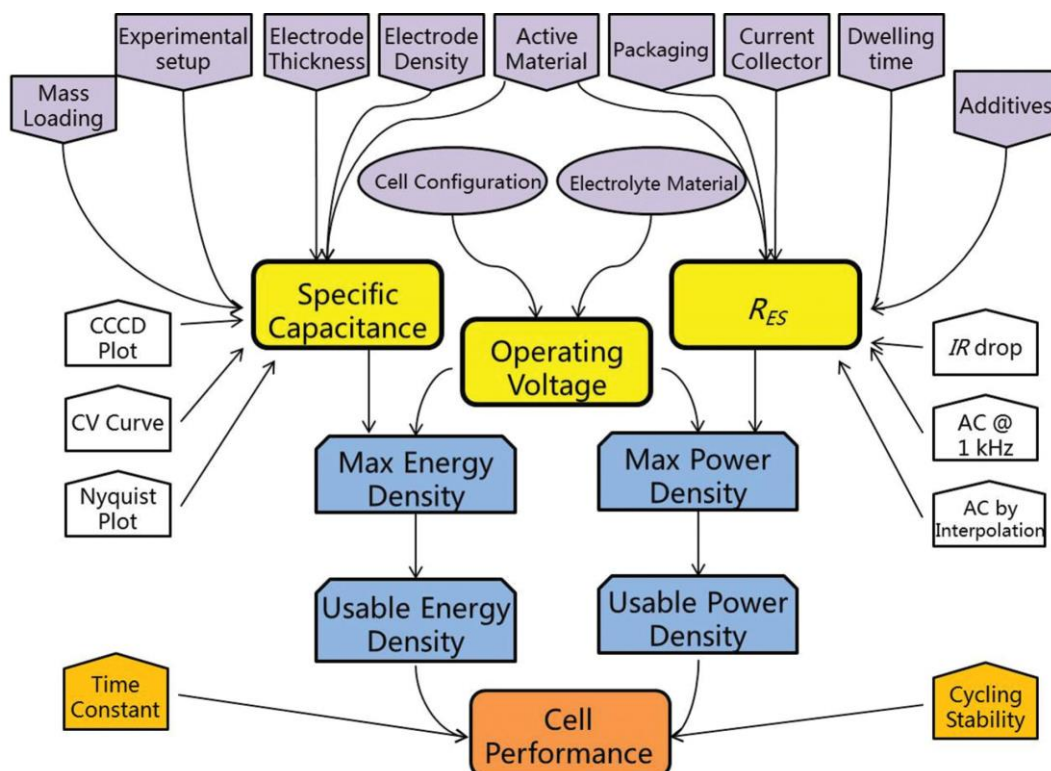


Figure 2-13: Major factors, metrics and test methods that are used for performance evaluation of SCs [46]

Figure 2-13 gives an illustration of the major factors, metrics and test methods that are used for the performance evaluation of SCs. The following sections will discuss about few of metrics and test methods.

2.4.1 Quality Assessment of CNT Materials

To evaluate the performance of the SCs few aspects of have to be taken into account. Firstly, the electrode materials, for instance CNT, need to be characterised to ensure that the desired materials are grown by the CVD process, the quality, and the material properties of materials. These can be done by the morphology of CNTs with different material characterisation tools. Morphology of CNTs plays a crucial role in their

performance as electrodes in SCs. The key aspects of CNT morphology that influence SCs applications include diameter, length, porosity, wall structure (single-walled or multi-walled), carpet height², purity, adhesion and alignment.

The diameter of CNTs affects their surface area and, consequently, the amount of charge that can be stored. Smaller-diameter CNTs generally have higher surface areas, providing more electrochemically active sites for energy storage. The length of CNTs influences transportation of charge and can enhance the mechanical integrity of the electrode material. Longer CNTs improve connectivity between the electrodes and reduce the chances of structural degradation during charge-discharge cycles. There is a concept of inter-connected cross-linked CNTs that was discussed before, which enhances charge transport and other properties of the CNTs in a positive manner [26], [27] Purity is crucial for optimal SC performance. Impurities, such as amorphous carbon or metal catalyst residues, can adversely affect the characteristics and potential toxicity of CNTs [47]. For this purpose, highly purified CNTs are desirable.

Porosity is another important parameter that is used for speculating how the SCs might behave under different electrolytes. It can affect the performance of the SCs by trapping air or other gases to block the pores for ion exchange. This makes it difficult for the ions to have the steady exchange of ions and thus leading to degradation of capacitance and other performance parameters.

Overall, optimizing CNT morphology, is important for speculating the performance of SCs. Morphology can be performed by scanning electron microscopy, transmission electron microscopy, Brunauer-Emmett-Teller (BET), Raman spectroscopy, Fourier-transform infrared spectroscopy (FTIR) and so on. SEM and TEM images can provide useful and detailed information about the diameter, thickness, length, and an overview of the growth of the CNTs. BET is used to for the active surface area of the CNTs, Raman and FTIR spectroscopy can detect the peaks that correspond to different bonds of carbon so as to ensure the existence of CNTs. There are other tools and techniques for the characterization of CNTs but those are out of the scope of this study. Figure 2-14 shows the SEM images of CNTs at different magnifications showing the interconnected cross-linking between CNTs.

² Cross-sectional height of the active area of CNT

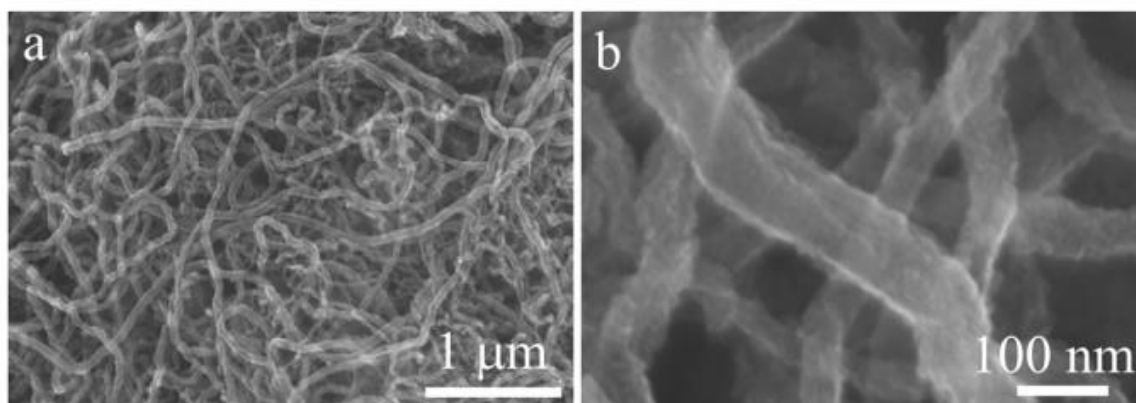


Figure 2-14: SEM images of interconnected and cross-linked fullerene-like carbon decorated CNT (FC-CNTs) [22]

2.4.2 Electrochemical Performance of SCs

For evaluating the electrical performance of the electrode³ and the whole cell⁴, different electrochemical characterization techniques are crucially important to be tested and analysed. A potentiostat is a device that controls the potential of the electrode and record the change in the electrode current and vice versa.

2.4.2.1 Three-electrode & two-electrode systems

For the electrochemical characterization the testing protocols can be configured into two parts: 1) Three-electrode system; and 2) Two-electrode system.

Three-electrode system is usually incorporated to find the performance of the electrode material. It is a faster technique and easy to implement and work with. In a three-electrode system there are working electrode (WE), reference electrode (RE) and counter electrode (CE). WE is the desired electrode material to be tested for e.g., CNT. WE is submerged into sufficient amount of electrolyte/solvent so that the active material on the electrode is in contact with the liquid. RE is usually used to as a base potential that has a fixed and stable potential itself. Commonly silver-silver chloride solution electrode (Ag/AgCl) is used as the RE. Finally, a CE maintains the electrochemical balance within the WE by modulating its potential. To fulfil this function, materials with high conductivity and inert characteristics, such as platinum meshes or graphite rods, are commonly used. A voltage is applied across

³ Only the electrochemical characterization of the electrode itself

⁴ Coin cell, pouch cell or any other cell format.

the WE and RE with a potentiostat and current is measured with WE and CE as shown in Figure 2-15 [45].

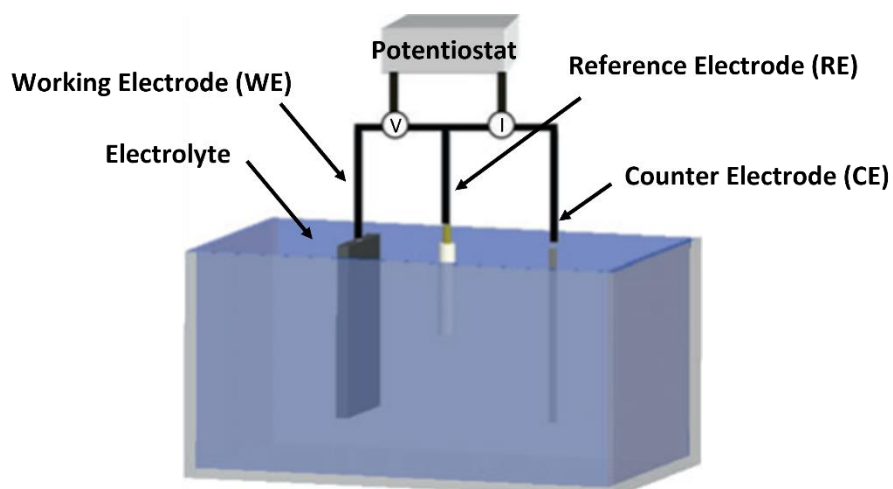


Figure 2-15: Three-electrode system showing WE, RE and CE [45]

On the other hand, a two-electrode system is usually incorporated for a whole device i.e contains a cathode and an anode. Coin cells and pouch cells are measured using two electrode setup. There are two terminals, one is connected with the cathode and the other to the anode of the device. The difference is that there is no RE like the three-electrode setup [45].

2.4.2.2 Test Methods

Several testing methods are implemented for the electrochemical characterisations of the SCs for its performance evaluation. Commonly used test methods are as follows: A) Cyclic Voltammetry (CV); B) Galvanostatic charge-discharge (GCD) & constant current charge-discharge (CCCD); and C) Electrochemical impedance spectroscopy (EIS). These methods are primarily employed for the measurement of key parameters including voltage, current, and time. These parameters serve as the basis for further calculations pertaining to capacitance, equivalent series resistance, operating voltage, power density, energy density, time constant, and other related quantities. These calculations provide valuable insights into the performance and characteristics of the system under investigation.

Cyclic Voltammetry (CV): CV technique is useful for the quantitative and visible data representation of the electrochemical behaviour of the active material. A potential is applied to the WE relative to the potential of the RE, creating a sweeping voltage profile

that oscillates within a predefined range determined by the user. The potential window depends on the electrolyte used as discussed earlier. The rate of the potential change is called sweep rate or scan rate and measure in mV/s or V/s. As the potential is applied, the instantaneous time dependent current is recorded and plotted as current (I) against potential (E). Schematic of CV curves for material configuration are shown in Figure 2-16. For a pure capacitive form of an EDLC the CV curve is of rectangular shape. The behaviour changes when there is the existence of pseudocapacitance, distorting the shape as shown.

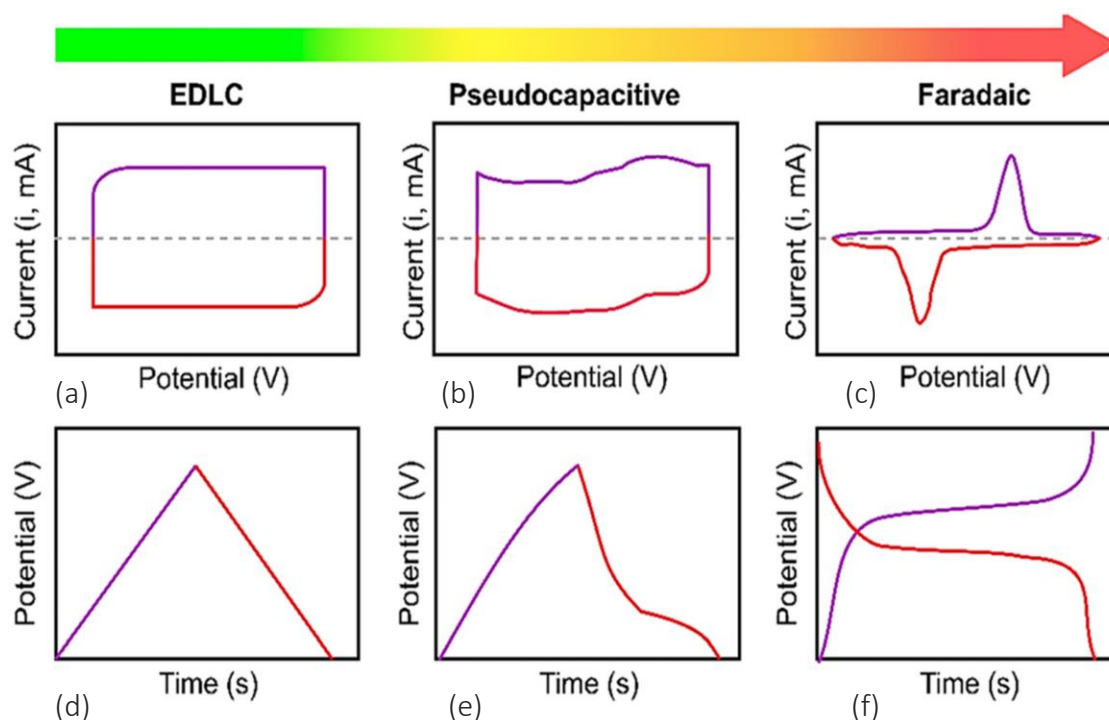


Figure 2-16: Schematic of (a-c) CV and (d-f) GCD curves for EDLC, PC and faradaic materials [48]

Galvanostatic charge-discharge (GCD) & constant current charge-discharge (CCCD):

GCD and CCCD both are widely used for the electrochemical characterizations of SCs. In these testing methods, a constant current is applied to (dis)/charge the SC up to a certain potential. Potential with respect to time is recorded and the output is a plot of potential (E) versus time (s). The charging and discharging current depend on the SC device. These testing methods can be used for measuring the important parameters capacitance, series resistance and operating voltage. Other parameters mentioned above can also be calculated from these techniques. Usually for an ideal EDLC the GCD curve, as shown in Figure 2-16, is a linear line from initial to peak potential and back to the initial again [45],

[46]. Both GCD and CCCD have the same working principles but only differ with the setting in the program, i.e., for CCCD different current can be applied with respect to time.

Electrochemical Impedance Spectroscopy (EIS):

It is a method of test that involves the application of a low amplitude alternative voltage, typically in the millivolt range, to maintain a steady-state potential. The impedance of the cell is then measured over a range of frequencies (0.01 Hz to 1MHz), providing valuable information about the electrochemical behavior and properties of the system under study. The output graph is a Nyquist plot in which imaginary and real impedance parts of the cell are plotted [45]. The utilization of frequency response characteristics serves as a valuable tool for examining electrochemical capacitors that incorporate electroactive electrode materials. Through this investigation, important insights are gained regarding various aspects, including:

- (a) The inherent electrode properties.
- (b) The distribution of pore sizes within electrode materials possessing a high surface area.
- (c) Criteria like the electrode thickness and the interaction between particles [7].

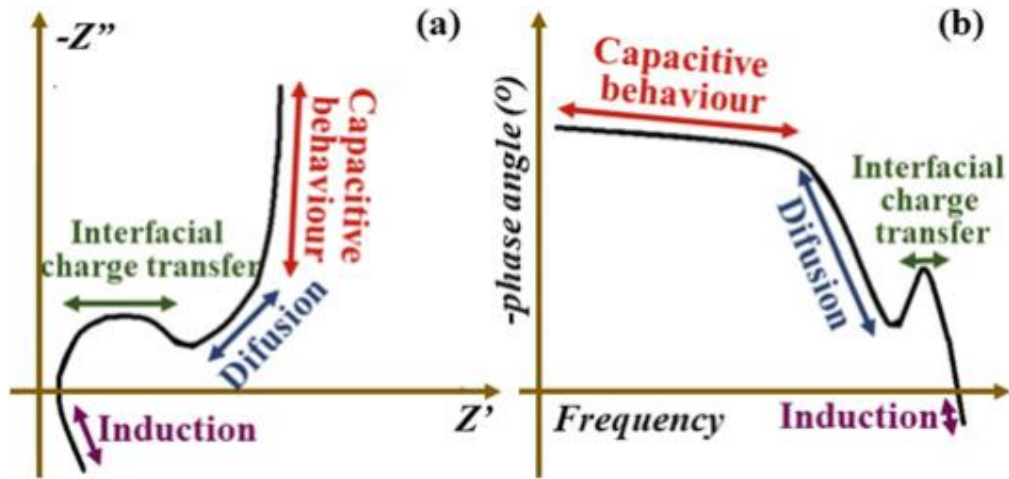


Figure 2-17: Schematic of a) Nyquist Impedance and b) Bode plot [7]

A general impedance model schematic is shown in Figure 2-17. There are few elements that are can be extracted from the Nyquist plot. The semicircle in the high frequency region depicts the ESR^5 (denoted as R_s) and the resistance due to charge transfer of the electrode

⁵ Internal resistance mainly contributed by electrolyte

material (denoted as R_{ct}). The resistance due to the diffusion behaviour of the electrolyte is represented by Warburg element. And finally, a slope or a line parallel to the imaginary plane represents the capacitive behaviour of the electrode or device [7], [49], [50]. All these elements can be simplified in a Randles equivalent circuit for SC circuit modelling, shown in Figure 2-18. Here C_{dl} is the electric double layer capacitance.

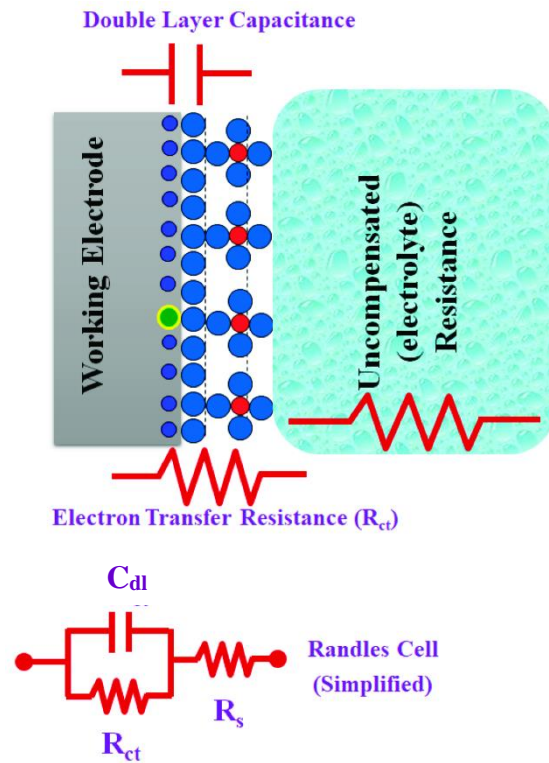


Figure 2-18: A simplified representation of a Randles circuit to depict EIS [49]

Therefore, EIS technique is a powerful non-invasive technique that can be used to interpret the behaviour and properties of SC material. EIS plays a crucial role in advancing the knowledge of electrochemical systems and facilitating the design and optimization of energy storage devices and electrochemical sensors.

3 Experimental Setup & Procedure

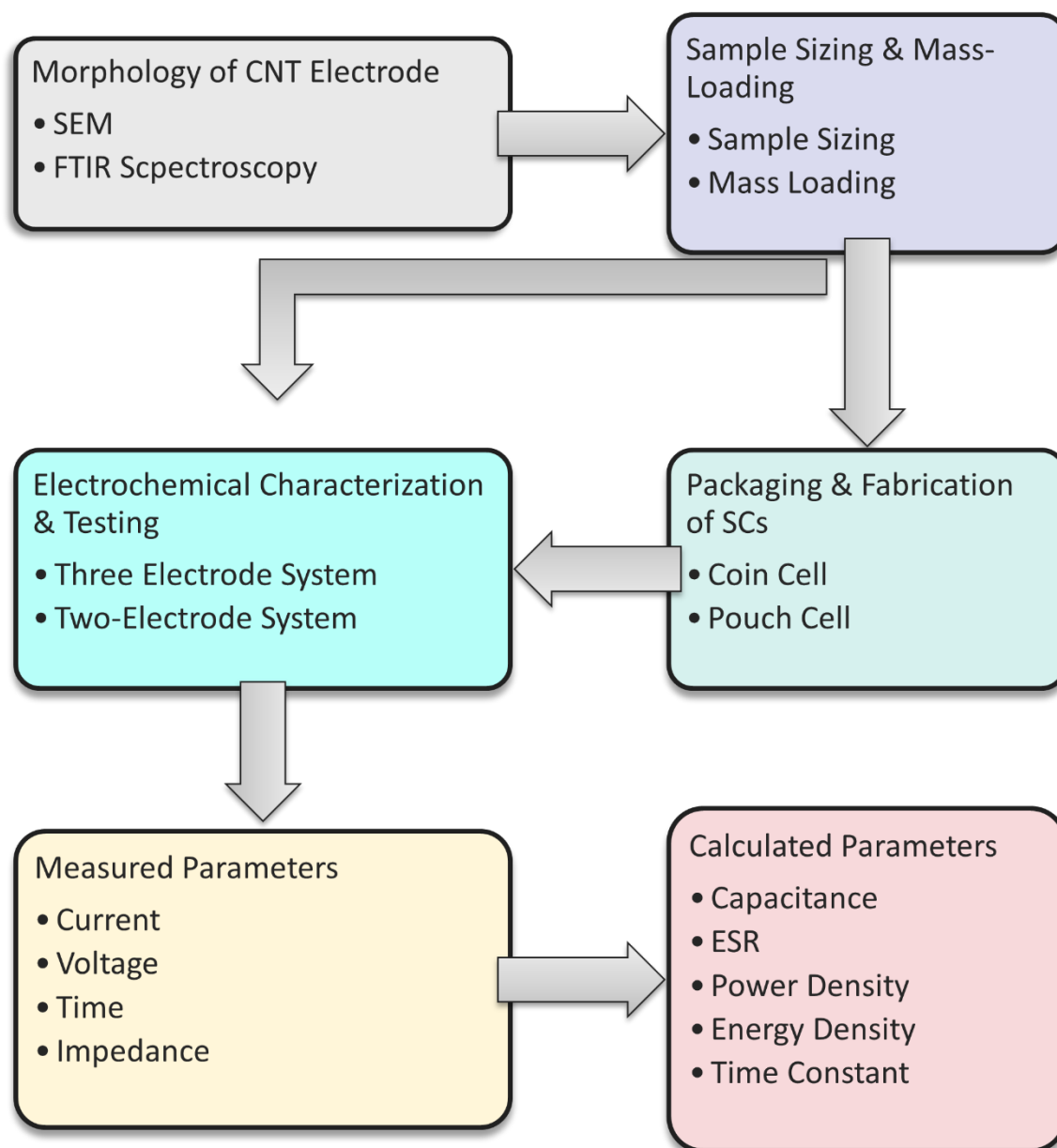


Figure 3-1: Flowchart of the experimental setup and procedure for this study

The experimental setup & procedure chapter in this thesis covers several important aspects of the research. Firstly, the morphology of the CNTs electrode is explored, providing insights into its structure and properties. Next, the sample sizing and mass loading for testing and assembly is detailed, outlining the steps taken to ensure the electrode's integrity and functionality. The chapter further describes the cell assembly process, explaining how the AI-CNT electrode and other components are assembled to form the electrochemical cell. Electrochemical characterization techniques are then

employed to analyze the performance of the cell, measuring parameters such as voltage, current, and impedance. Furthermore, calculated parameters are derived from the measured data, which includes parameters like capacitance, ESR, energy density, power density etc. This comprehensive experimental setup and procedure chapter establishes a solid foundation for the subsequent analysis and discussion in the study. Figure 3-1 gives a thorough overview of the different experimental setup and procedures incorporated in this study.

3.1 Morphology & Material Characterisation of CNTs Electrodes

The Al-CNTs electrodes used for this study was fabricated using technology invented by the researchers of University of South-Eastern Norway [25], [51]. The Al-CNTs electrodes were received after the growth by APCVD process.

After the growth of the CNTs the samples are extracted and ready for the next steps of material and electrochemical characterisations. Figure 3-2 demonstrates the images of typical samples before (left) and after (right) the growth of CNTs.



Figure 3-2: Typical samples before and after the growth of CNTs

Characterizations of the samples were conducted through SEM (Hitachi SU3500) and Field Emission SEM (FE-SEM, Hitachi SU 8230) (see Annexes). In this study, the utilization of both SEM and FE-SEM allows for the generation of high-resolution images of the sample's surface. This enables precise observations of the nanoscale structure of CNTs comprehending their morphology, diameter, length, and other relevant characteristics. Assessing the quality, uniformity, cross-linking and to make an idea about the thickness of the Al-CNTs electrode are of importance in this research, and the capabilities of SEM and FE-SEM play a vital role in achieving this objective.

In this study, FTIR (Nicolet iS50, Thermo Fischer) (see Annexes) with a 1064 nm laser as the excitation source and a maximum power of 0.5 W was utilized to detect the presence of CNTs and/or amorphous carbons. The operational principle of FTIR involves analysing the sample's absorption of infrared radiation across different wavelengths. The absorption of infrared light by different functional groups and bonds present in the samples produces a unique spectrum, which can be used for quantification and identification purposes. By examining the distinctive FTIR spectrum, the existence of CNTs and amorphous carbons can be identified and quantified.

3.2 Packaging and Fabrication of Supercapacitors

3.2.1 Sample Sizing & Mass Loading Measurement

Mass loading was to accurately determine the mass of the grown CNTs in this study. It is worth mentioning that the area of the substrate was also measured to get the mass loading of the specific parameter in milligram per square centimetre (mg/cm^2). To accurately find the carpet weight or mass loading of the CNTs, the mass of the foil and the Ni loading were subtracted from the final mass loading with all the material after growth. Eq. (9) shows the formula used to determine the mass loading of CNTs.

$$M_{CNT} = M_{After\ growth} - M_{Before\ growth} \quad (9)$$

Here M_{CNT} is the carpet weight or mass loading of only CNT in mg/cm^2 .

After the mass loading, electrodes were cut into particular size for the electrochemical test and assembly. To make the calculation more precise, each of the sized electrodes' mass loading was also performed. Importantly that for the three-electrode system of measurement only the CNTs electrode itself was required. This means that no assembly or packaging was needed to perform the three-electrode test. For three-electrode test setup, samples were cut into 1 cm^2 size to have consistency in the measurement. The three-electrode system measurement was used to have a quick understanding of the performance of the electrode. Later, from the same sample coin cell and pouch cell electrodes were taken.

For the coin cell assembly, electrodes were die punched with a hammer in circular disks. The size of the die has a diameter $\varnothing=11$ mm and this size was used throughout. Each circular disk has an area of ~ 0.95 cm². 11 mm diameter was used because it is much closer 1 cm² as the electrode area. This was done to make consistency in electrode dimensions between the different assembly configurations. Glass fibre separator- MN GF-5 GF/F (Macherey-Nagel [14]) of thickness 0.4 mm was used for coin cell. The separator needs to be larger than the electrode size to avoid short circuit or contact between the electrodes, so $\varnothing=16$ mm circular disk was used. This glass fibre separator was chosen because it has a higher electrolyte retention capability, chemically resistant towards organic and inorganic electrolyte, easier to handle inside glovebox and can withstand temperature [14].

For the pouch cells, two sizes of electrode dimensions were used: a) 1 cm² and b) 2 cm². This means that for few pouch cells 1 cm² electrode dimension was used and for few it was 2 cm². The calculations were normalised by the area of the electrode. Same separator was used for the pouch cell, but the dimension was taken 1.5 times the area of each electrode. It is to be noted that, regardless of the configurations both the electrodes (cathode and anode) inside a specific cell have the same dimension. Figure 3-3 shows a picture of the glass fibre separator used for this study.



Figure 3-3: Glass fibre separator used in this study [14]

Packaging of the SCs have several steps to follow. Supercapacitor organic electrolyte CF4531 with 25 wt.% N,N-Dimethylpyrrolidinium-Tetrafluoroborate (DMP-BF₄) dissolved in 75 wt.% acetonitrile (ACN) was used for this study. This organic electrolyte, DMP-BF₄, was chosen because it has superior performance in terms of operating potential window and stability. For its good performance, this electrolyte is used for research as well as for

industrial purpose. More details about the performance of DMP-BF₄ are mentioned in the previous section.

3.2.2 Coin Cell Packaging

For coin cell packaging and assembly, CR2032 (Gelon SS304) coin cell parts were used. Spacer has a thickness of 1.0 mm and diameter of 16.0 mm. The electrode disks are labelled properly and then taken into the N₂ filled glovebox (EasyLab, MBraun) for the assembly.

The assembly is done inside the glovebox for several reasons:

- a) To ensure a highly purified atmosphere and very low levels of oxygen and moisture
- b) Prevents the contamination of sensitive components within the coin cell, such as the electrolyte and electrodes, by moisture, oxygen, or other impurities present in the ambient air.
- c) Eliminates the risk of undesired reactions and ensures the safety of the assembly process.
- d) The organic electrolyte is volatile and evaporates very quickly in normal atmosphere.

The electrodes, separator, and electrolyte all are put inside the coin cell parts as mentioned in chapter 2.3.1. An approximation of the thicknesses of the electrodes from SEM cross-section was made to make an idea for the volume of electrolyte. Using a pipette, electrolyte volume of 80 μ L was used for each cell. Digital electric crimper (MSK-160E, MTI Corporation [52]) was used for the coin cell crimp pressure. Pressure of 0.6-1.4 T⁶ labelled in the crimper was used in this study for the coin cell assembly. Figure 3-4 shows the different coin cell parts for the packaging before and after assembly. After the assembly the coin cells are cleaned and rubbed in tissue paper with distilled water and labelled. Height of the coin cells after assembly is approximately 3.0 mm.

⁶ 1 T= 1 Kilogram per sq. inch = 6.90 MPa

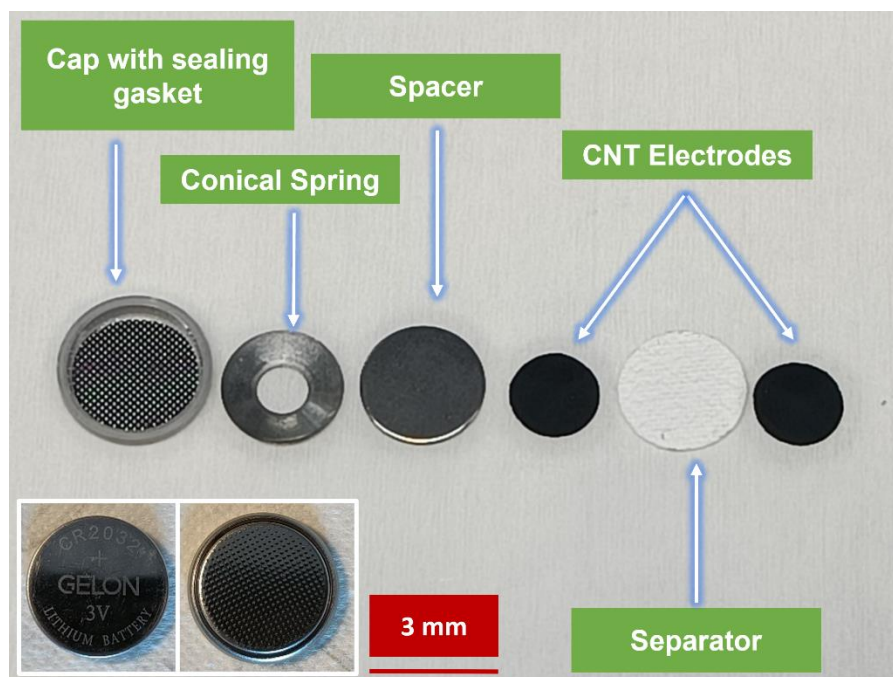


Figure 3-4: Images of coin cell parts before and after packaging

3.2.3 Pouch Cell Packaging

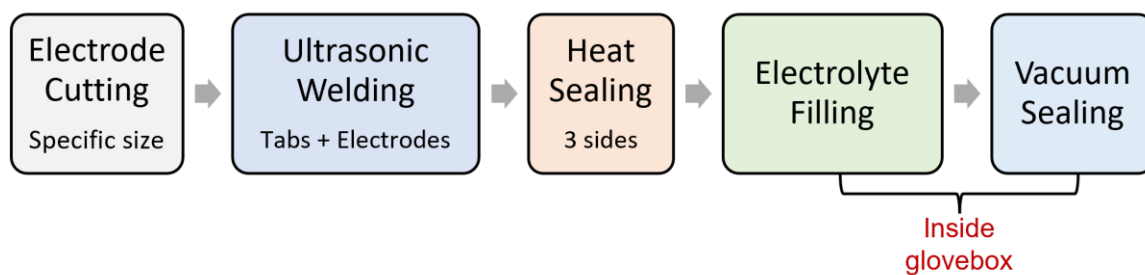


Figure 3-5: Pouch cell packaging steps

Pouch cell packaging steps and pouch cell configuration are shown in Figure 3-5 and Figure 3-6 respectively. First the electrodes are cut into specific sizes. Next, the electrodes are electrically connected with the Al tabs using ultrasonic welding tool (MWX 100, Branson) with energy input of 10 J, while the power and time was set automatically set by the program.

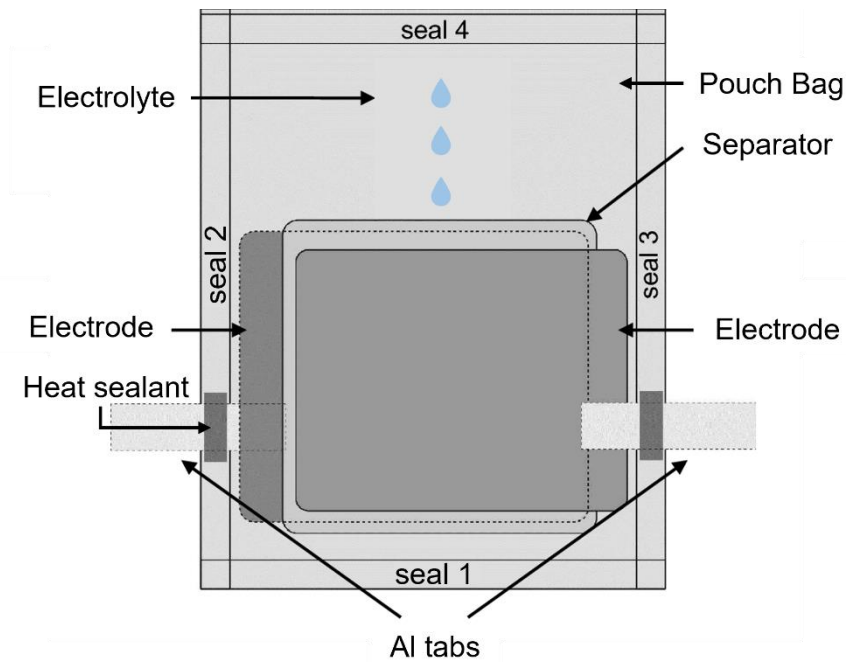


Figure 3-6: Pouch cell configuration showing the components and sealing positions

Pouch bags were cut according to the size of the electrode and were heat sealed using hot gun (KMS technologies) on one side labelled as seal 1. The first sealing was done this way. Separators were placed inside the drying oven (Binder) for at least 12 hours at 80 °C to remove any moisture. Next, the welded electrodes-tabs were put in place so that the tabs reach outside the pouch bag for terminals. Both the electrodes-tabs were aligned properly to keep the heat sealant⁷ just on the edge of the pouch bag and a separator was put between the electrodes. Now, both the sides of the electrode-tabs were heat sealed with the pouch bag (seal 2 and 3). At this stage only the seal number 4 is remaining. Afterward, the pouch cell was taken inside Ar filled glovebox (LabMaster, MBraun) for electrolyte filling and vacuum-heat sealing. About 120 μ L and 250 μ L of electrolyte were used for 1 cm² and 2 cm² sized electrode respectively. Now that electrolyte filling was done the pouch cell was ready for the final sealing. The cell was placed inside the vacuum-heat sealer (KMS technologies) and vacuum was applied for 30 seconds to remove the air out of the pouch bag. The 4th sealing was done, and the pouch cell was then ready for testing. Labelling was done to distinguish the cells.

⁷ Consist of thermal bonding film

3.3 Electrochemical Characterisation and Testing

Electrochemical characterisations and testing were done using three-electrode system and two electrode system to measure different parameters of CNTs electrode SCs.

3.3.1 Three-electrode & Two-electrode test

As mentioned previously, for three-electrode system, Al-CNT electrode was directly used for the test. Three-electrode test was assembled to characterize the electrochemical behaviour of single electrode. Figure 3-7 shows an overview of the components and connection for the three-electrode setup. Al-CNT electrode sample is cut into specific dimension and attached with the WE of the setup. Graphite rod is used as the CE and Ag/AgCl solution (in saturated KCL) was used as the reference electrode. The electrolyte for used for this test was 1 M Na_2SO_4 (CAS-No.: 7757-82-6, Sigma-Aldrich) aqueous solution. The terminals of WE, CE and RE all were connected to the potentiostat i.e., electrochemical workstation (VMP3 & VSP-300, BioLogic).

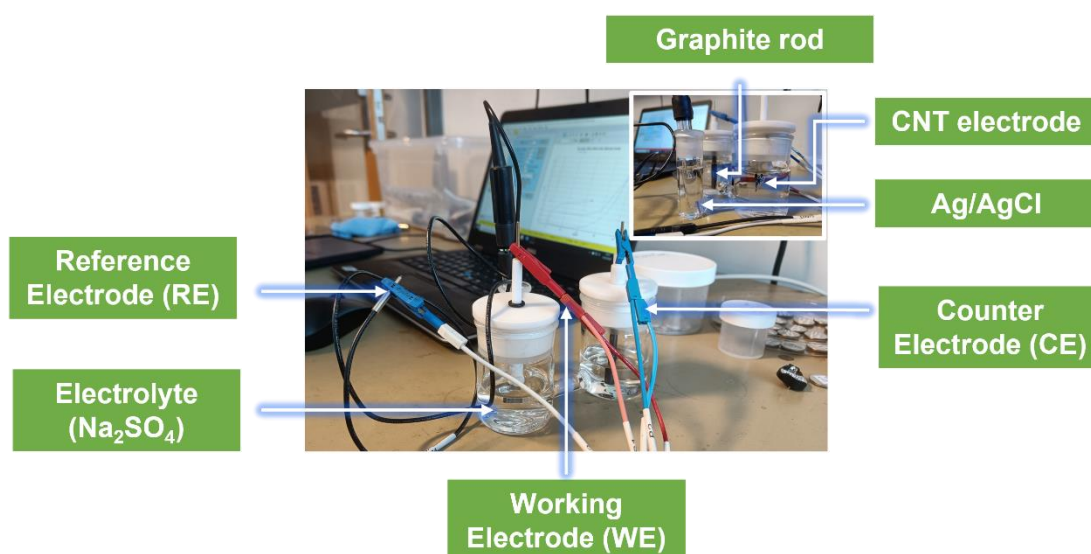


Figure 3-7: Assembly setup for three-electrode system

The potential window for the three-electrode test were set 0-0.8 V. Decomposition potential is observed beyond this value, so this potential limit was chosen [53]. Electrochemical measurements by CV, GCD, EIS, CCCD and cyclic stability test were performed using EC-Lab, which is a software for controlling the BioLogic potentiostat.

Different programs are set in EC-lab according to the requirement and tests data are recorded and saved by the software.

Coin cells and pouch cells are tested with two-electrode test setup. In a two-electrode test setup, there are only two electrodes involved: a positive electrode (anode) and a negative electrode (cathode). For this study, both the cathode and anode are of the same material i.e., CNTs based electrode. They can be called symmetric coin/pouch cell SC. This means that there are no specific positive or negative terminal for the connection. Figure 3-8 demonstrates the test setup for coin cell and pouch cell. There are two connections for cathode and anode.

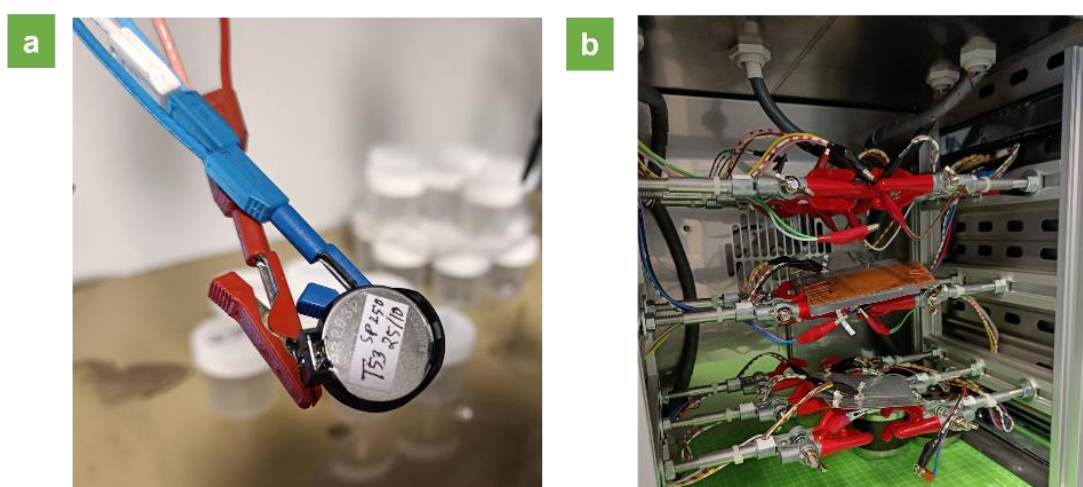


Figure 3-8: Test setup for a) coin cell and b) pouch cell

A stable operating potential window was determined by applying potential of 2.0 V to 3.0 V. The operating window varied with the type of CNT sample. Cells were run at different temperatures of -20 °C, 25 °C and 60 °C to investigate the performance of SCs under different physical conditions.

All the tools used are shown in Annexes.

3.3.2 Calculations for Parameters

3.3.2.1 Capacitance

For a SC with two electrodes if the capacitance can be expressed as C_1 and C_2 , the total capacitance (C_T) for a SC device can be put into equation as:

$$C_T = \frac{1}{C_1} + \frac{1}{C_2} \quad (10)$$

As C_1 and C_2 both are same for symmetric SC, C_T can be expressed as:

$$C_T = \frac{1}{2} C_E \quad (11)$$

Where C_E is the electrode capacitance.

From CV technique, capacitance can be calculated by the following equation:

$$C_E = \frac{\int idV}{2V_s \Delta V \Pi} \quad (12)$$

Where $\int idV$ is the area under curve from CV, i is the constant current, V_s is the voltage scan rate, ΔV is the potential range and Π can be the mass loading of the active electrode or the surface area of the electrode material. Thus, the normalised or specific electrode capacitance, C_E , can have the units $F\text{ cm}^{-2}$ or $F\text{ g}^{-1}$. The former is called specific areal capacitance while the latter is called gravimetric capacitance.

From GCD technique, capacitance can be calculated as follows:

$$C_{GCD} = \frac{I \Delta t}{\Delta V \Pi} \quad (13)$$

Where I is the applied current, Δt is the discharge time, ΔV is the discharge voltage and Π can be the mass loading of the active electrode or the surface area of the electrode material. Equations used above are taken from these references [7], [9], [45], [46].

3.3.2.2 Energy Density

The energy density can be calculated from the following equation:

$$E = \frac{1}{2} \frac{C_{T/E} (\Delta V)^2}{3.6 \times \Pi} \quad (14)$$

Here $C_{T/E}$ is the capacitance of the total device or only the electrode, Π can be the mass loading of the active electrode or the surface area of the electrode material and ΔV is the operating voltage [9], [45], [54]. Unit of energy density can be written as Watt-hour per sq. cm, Wh/cm^2 or as Watt-hour per kilogram, Wh/kg .

3.3.2.3 Power Density

The term specific power density, expressed in Watt per kilogram W/kg or Watt per sq. cm W/cm^2 , refers to the rate at which a device can efficiently supply energy to external

loads while maintaining a consistent current density. Therefore, maximum specific power density, P , can be expressed as [9], [45]:

$$P_{max} = \frac{(\Delta V)^2}{4\Pi R_{ESR}} \quad (15)$$

Where ΔV is the operating potential, Π can be the mass loading of the active electrode or the total mass of the device and R_{ESR} is the ESR of the cell.

3.3.2.4 Equivalent Series Resistance (ESR)

Equivalent series resistance (ESR) is an essential parameter when it comes to SC application. It is even more important when there is a need for pulse power application. The reason lies in the fact that ESR is inversely proportional to power, so lower ESR means higher power. So, to get a higher power density it is essential to use an electrolyte with high ionic conductivity. Although organic electronic has a larger potential window, but the ionic conductivity is lower than aqueous electrolyte. In this regard, a compromise is there between operating voltage and ionic conductivity. Also, ESR is related to the time constant, τ , that indicates a device's responsiveness for charge time that will be shown in the next sections.

As discussed previously, to get the Nyquist impedance plot, a small perturbation of 1.5mV from 1 MHz to 0.1 Hz was applied. Data were recorded as complex imaginary impedance and real impedance in the y and x-axis respectively. A semi-circular curve is usually obtained and ESR can be measured from the curve. ESR can be obtained from the curve in two ways:

1. The real impedance value of the curve just crossing the x-axis, and
2. By measuring the real part impedance at 1kHz.

EIS curves can be fitted to different equivalent circuits and various parametric values representing electrolyte-electrode-current collector resistance, EDL capacitance, diffusion resistance (Warburg element), non-ideal capacitances due to porosity and non-homogeneity etc.

3.3.2.5 Time constant

Time constant for a SC is represented by τ and can be defined as[46]:

$$\tau = R_{ESR}C_T \quad (16)$$

Where R_{ESR} is the ESR and C_T is the total capacitance of a SC cell. A smaller value of τ indicates a higher level of responsiveness for the device. In the case of most commercial SCs, the typical range for τ is between 0.5 and 3.6 seconds [46].

4 Results and Discussions

This chapter will provide the results and the detailed analysis of the studies done for this thesis. Data are represented with images, graphs, charts, and tables. Supplementary data are listed in Annexes.

4.1 Morphology & Analysis of CNTs Electrodes

FE-SEM images of CNTs electrodes with different Ni loadings can be seen in Figure 4-1. The “dense forest” of CNTs can be observed from the images. The growth of the CNTs depends on the type of Ni loading, Ni deposition technique, Ni particle thickness and growth mechanism of the Ni particle or cluster [55] on the substrate (Al). Therefore, it affects the adhesion, diameter and length of the CNTs.

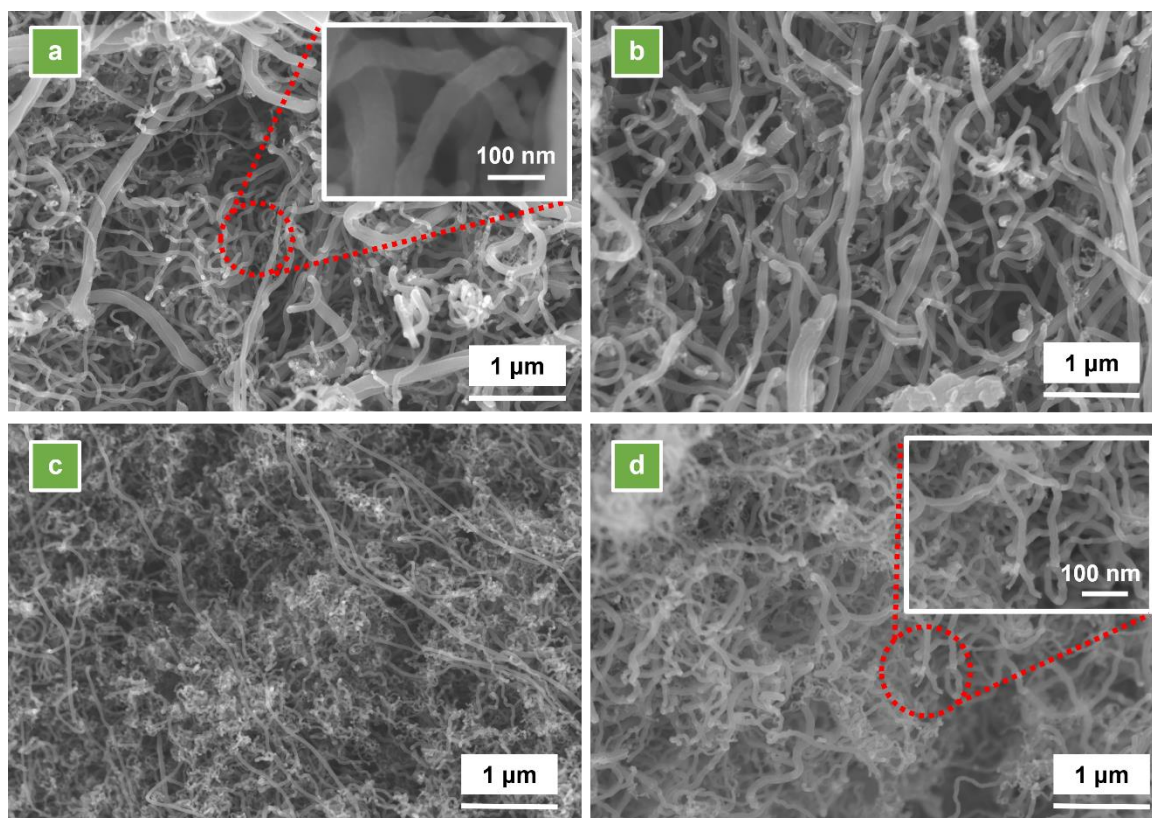


Figure 4-1: FE-SEM images of CNTs with different Ni loading type, a) with Ni sputtering; b) NiSO₄ solution dip coated; c) NiSO₄ spray coated and d) NiSO₄ drop coated

From Figure 4-1 a, Ni sputtering loaded CNTs can be seen which reveal its existence in spaghetti-like morphology. The diameter of the CNTs had a variation from 38 nm – 146 nm. The variation in diameter is due to the size of the Ni particle/cluster growth while

sputtering as investigated by other researchers [56]. For CNTs grown from sputtered Ni loading, the growth of CNTs is heavily influenced by the tip growth mechanism as sputtering process is non-conformal and thin film deposited by this process are mostly concentrated on the surface [55], [56]. In case of the NiSO₄ solution samples (dip, drop, spray coat, see Figure 4-1 b, c, and d), the CNTs are predominantly smaller in diameter. CNTs grown from dip coated NiSO₄ had a diameter distribution of 31 nm – 91 nm and for spray and drop coated the diameter range was 28 nm- 136 nm. The cause of the smaller diameter with the different types of NiSO₄ solution coating is due to the Ni particle size. In the presence of sulphur content in the NiSO₄ solution, the particle size of the catalyst decreases which results in smaller diameter, enhanced growth and dense area of CNTs [57]. A thorough investigation of CNTs growth by Tasfia *et al.* [3] with NiSO₄ solution coating as the catalyst chemical, demonstrated promising results in terms of mass loading of active material and SC performance. Therefore, the FE-SEM images serve as a logical proof of the existence of CNTs in the samples used for this study.

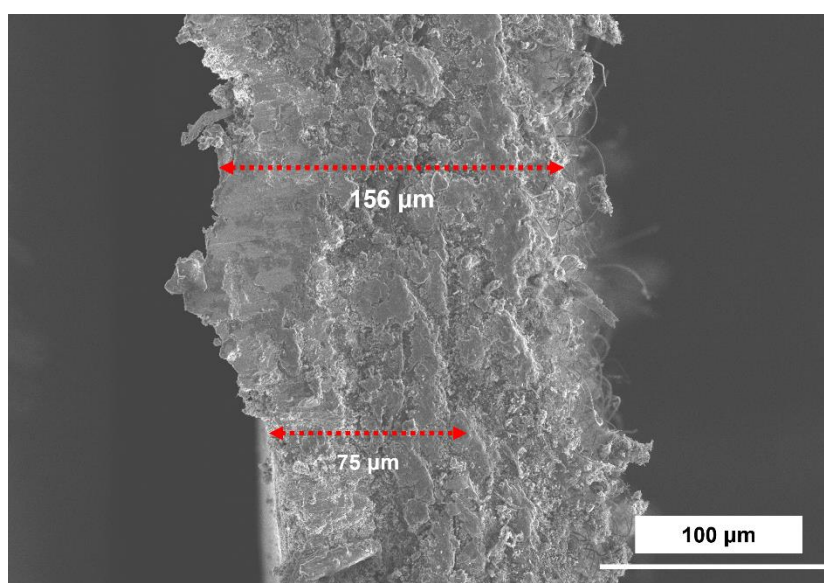


Figure 4-2: SEM cross-section of a Al-CNT sputtered sample showing thickness of the electrode

Figure 4-2 shows the SEM image of cross-section of a sputtered sample. It was done to make an approximation of the thickness of the electrode that was helpful for the electrolyte volume determination for packaging. From the image it can be observed that total thickness is around 156 μm that includes the foil thickness of ~75 μm. From the datasheet the foil thickness is mentioned 70 μm.

An idea of the porosity of the surface can be made from SEM images, though it is not an ideal tool for that, which helps to speculate the surface reaction of the electrode when assembled to compact packaging. Surface porosity of the electrode is a parameter that helps to speculate the behaviour of the electrolyte ion adsorption and exchange onto the electrode. It can also trap air bubble or residual gas from the CVD reaction which can affect the SC performance. So, the CNT morphology heavily influences the performance of SCs. To further investigate the presence of “only CNTs” and not any other carbon derivatives (for e.g., amorphous carbon), FTIR spectroscopy was performed for the same samples studied in SEM. Peaks at 744 cm^{-1} , 760 cm^{-1} , 598 cm^{-1} , and 750 cm^{-1} were observed for sputtered, dip coat, spray coat and drop coat, respectively (shown in Figure 4-3).

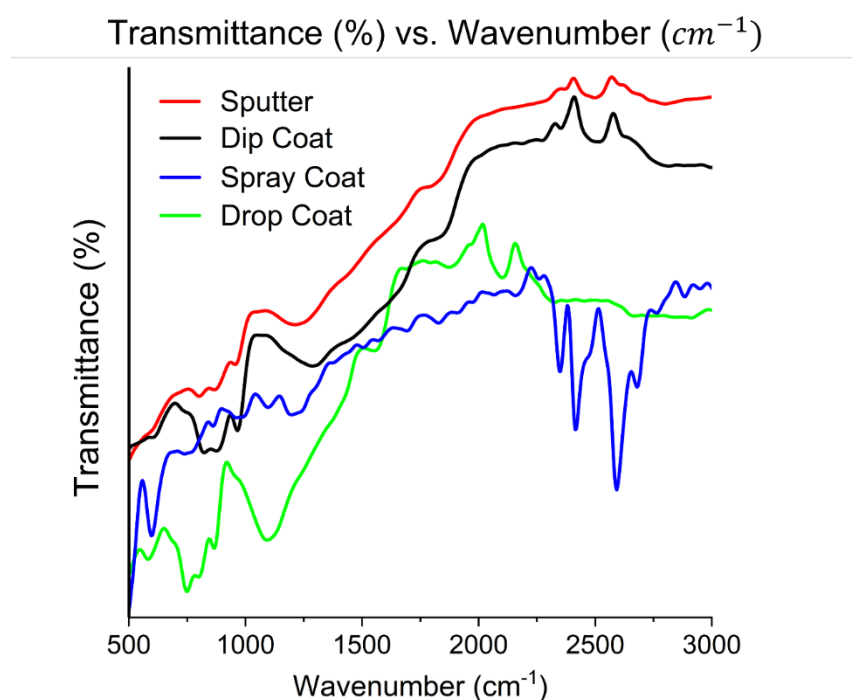


Figure 4-3: FTIR spectra of CNTs with different Ni loading, a) with sputtering; b) NiSO_4 dip coated; c) NiSO_4 spray coated and d) NiSO_4 drop coated

For all the four samples, peaks were identified between band $500\text{-}1000\text{ cm}^{-1}$ that represents the backbone of CNTs originated from the sp^2 hybridization of [58]. For sputtered sample there is a peak at $\sim 1205\text{ cm}^{-1}$ and drop coated sample there is a peak at 1560 cm^{-1} that also corresponds to the CNT backbone [58]. These analysis from FTIR spectra reveal the strong presence of CNTs.

4.2 Effects of Physical & Test Parameters on Supercapacitor Performance

The effects of different physical parameters on the performance of SC are presented and analysed. To make things easier to understand the type of samples, few tags are employed for the Al-CNT electrodes:

- CNT-SP: Growth of CNTs on Al substrate with *Ni sputtering*,
- CNT-DP: Growth of CNTs on Al substrate *dip coated* with NiSO₄ solution,
- CNT-SR: Growth of CNTs on Al substrate *spray coated* with NiSO₄ solution and
- CNT-DR: Growth of CNTs on Al substrate *drop-coated* with NiSO₄ solution.

If more than one sample of each of the above type is mentioned then it will be named as for e.g., CNT-SP1, CNT-SP2 and so on.

4.2.1 Analysis of Al-CNT Electrodes with Different Ni Loading

For the analysis of Al-CNTs electrodes with different Ni loading, four samples from the same APCVD experiment were tested and they are labelled as:

- CNT-SP1
- CNT-DP1
- CNT-SR1
- CNT-DR1

Nomenclature was mentioned before this chapter. To begin with, mass loading of each of the sample was done before the tests and assembly. Initially, three-electrode test was performed, and then coin/pouch cell packaging was done. Voltammograms (at 100 mV/s scan rate) from both the tests are shown in Figure 4-4. From both the graphs it is evident that CNT-DR1 sample shows higher current, but a very large redox peak is observed in the coin cell test. The reason for such high redox peak maybe due to the Faradaic reactions involved in the process. This causes the cell to show pseudocapacitive behaviour and have a profound peak. There are other possible reasons that might cause this behaviour, such as potential window and cyclic stability. If the potential window is more optimised, the curve can show good capacitive rectangular shape similar to other samples. In addition, more CV cycling can be done to minimise the redox peak. However, CNT-SP1, CNT-SR1 and

CNT-DP1 samples have good cyclic capability as can be seen from the graphs. Here it is important to note that, NiSO₄ solution was used for coating the surface in different ways. Usually, in the presence of sulphate enhances the growth of the CNTs as mentioned earlier. But with different method of coating (dip, drop, spray) the Ni loading might vary. Previous research [3] showed that CNT samples with drop coating exhibited excellent performance achieving specific capacitance per area or areal capacitance up to 2500 mF/cm². So, this result from the drop coated sample is consistent with the earlier findings.

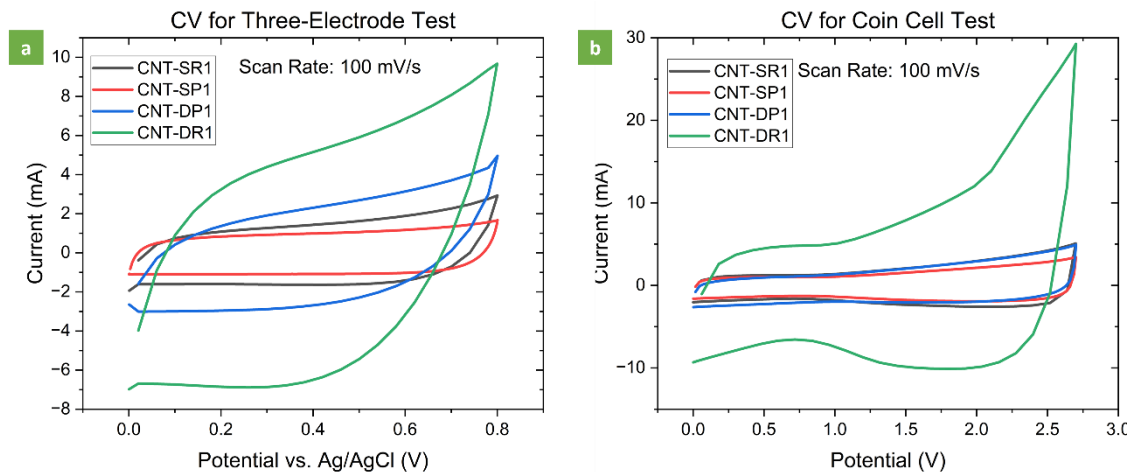


Figure 4-4: a) Three-electrode and b) coin cell measurement for four different Al-CNT samples

Data for capacitance and mass loading are demonstrated in Table 1 and plotted in Figure 4-5. From the data there is a clear trend in the increase of capacitance with the increase of mass loading of the active electrode material, which is expected, although with exception from CNT-SR1 sample. CNT-DR1 had the highest specific capacitance both for the three electrode and coin cell measurement 41.1 mF/cm² and 173.5 mF/cm², respectively. So, higher mass loading (per sq. cm) results in higher areal capacitance [59] which is needed for compact packaging of SCs where the application demands less area with more energy and power density.

Table 1: Data for different CNT sample showing capacitance and mass loading

Sample Type	Specific Capacitance- Three Electrode (mF/cm ²)	Specific Capacitance- Coin Cell Electrode (mF/cm ²)	Mass Loading (mg/cm ²)
CNT-SR1	12.9	43.6	1.62
CNT-SP1	7.98	32.9	3.76
CNT-DP1	13.8	41.3	5.44
CNT-DR1	41.1	173.5	9.10

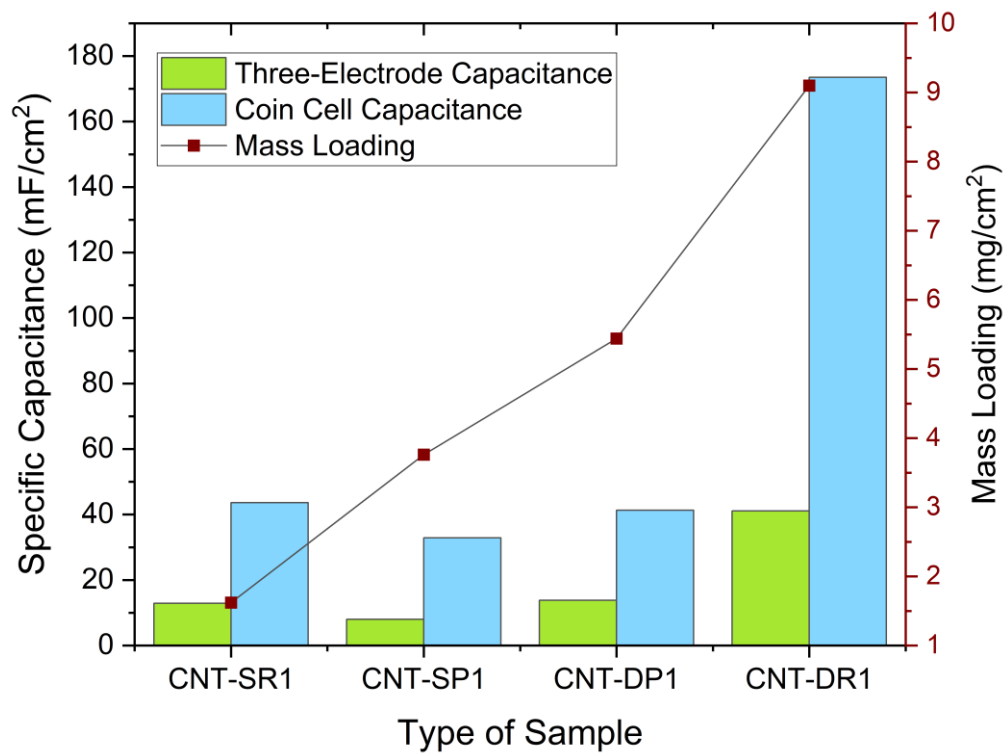


Figure 4-5: Bar chart showing influence of mass loading & type of CNT sample on areal capacitance

Although CNT-SR1 had a lower active mass loading but the areal capacitance was really good (43.6 mF/cm²) with high gravimetric capacitance of 26.9 F/g. This reveals the good properties in terms of both power density and energy density. For compact packaging this is much sought out for because of its capability of having high areal capacitance with lower mass which leads to lower device weight, increasing the energy density. Detailed analysis

of energy and power density for Al-CNTs based SC and how they effectively influence the performance of SC device will be demonstrated in the later sections.

It is also to be noted that with only three electrode test one cannot make a decision on the capacitance of the device. Compact packaging of SC in hermetic sealed condition can provide reliable information about the data of capacitance and helps to speculate the performance of the SC as a device.

4.2.2 Three-Electrode Tests & Analysis of CNT-SP2 and CNT-SP3

Tests using the three-electrode was done for the sample CNT-SP2 (shown in Figure 4-6) that was also utilized to package coin cell and pouch cell, described in the later section. Initially, the three-electrode test was done because it is a faster analysing technique to assess the performance of the SC electrode. From the CV curves shown in Figure 4-6, electrode capacitance at 100 mV/s was found to be 5.66 mF/cm² and for 5 mV/s it was 23.5 mF/cm².

Three-electrode measurement was done for another sample, CNT-SP3 (Figure 4-7). The CV plot clearly depicts the cyclic behaviour and demonstrates that the current exhibits a gradual change in response to voltage variations, after a sharp transition at the initial stage. This observation highlights the capacitive nature of an EDLC, where voltage influences the capacitance [6]. Data from different scan rates are shown in the CV curves (Figure 4-7 b)). At lower scan rates the capacitance becomes higher, this is owing to the sufficient penetration time of the electrolyte ions into the porous area of the CNTs. For the charge storage, the porous structures of the CNTs provide higher SSA to the ions and thus contribute to higher specific capacitance of SC electrode. On the contrary, at higher scan rates the electrolytes get less time to diffuse into the electrode surface for the charge

storage, thus resulting in lower capacitance. Figure 4-7 b) approves of the mentioned phenomenon depicting the effect of specific capacitance with scan rate.

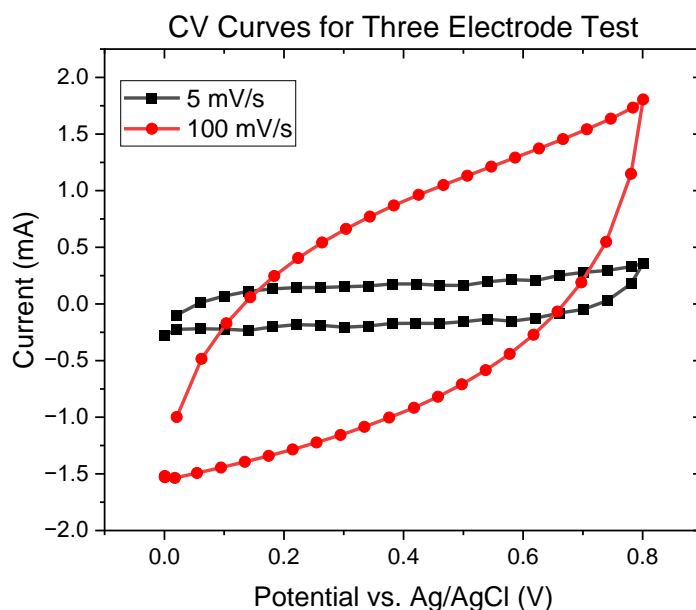


Figure 4-6: CV curves for three-electrode measurement for CNT-SP2

Although the potential window is lower for three-electrode test, the performance of only the electrode material itself can be investigated with such setup.

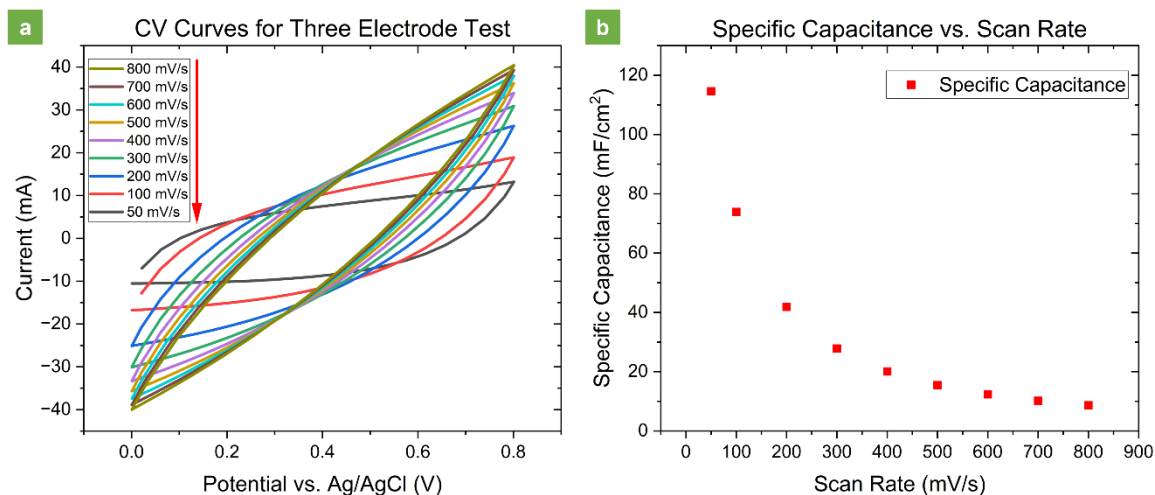


Figure 4-7: Three-electrode measurement a) CV curves; and b) effect of scan rate on capacitance for CNT-SP3

These tests were done to speculate the performance of the Al-CNTs electrodes before moving to the coin cell or pouch cell assembly. The same samples were used for coin and pouch cell, that will be discussed in the upcoming sections.

4.2.3 Effect of Temperature and Packaging Configuration

To investigate the performance of SC in different temperature conditions and package configuration, pouch cell and coin cell were tested and analysed. Different electrochemical tests were conducted for the same pouch cell under certain temperatures of $-20\text{ }^{\circ}\text{C}$, $25\text{ }^{\circ}\text{C}$ and $60\text{ }^{\circ}\text{C}$. Test of CV was done at 100 mV/s and 10 mV/s for pouch cell at the mentioned temperatures. Same pouch cell was put at different climate chamber for the electrochemical measurement. For the coin cell the same tests were conducted at $25\text{ }^{\circ}\text{C}$ but not at other temperatures like pouch cell due to limited lab resources. Potential window of 0 V - 2.7 V was selected for the tests for both the cell configurations. The coin cell was also included in the analysis because all the cells were made using the same sample and a comparison can be made in terms of the configuration. CNT-SP2 sample was used for both coin cell and pouch cell.

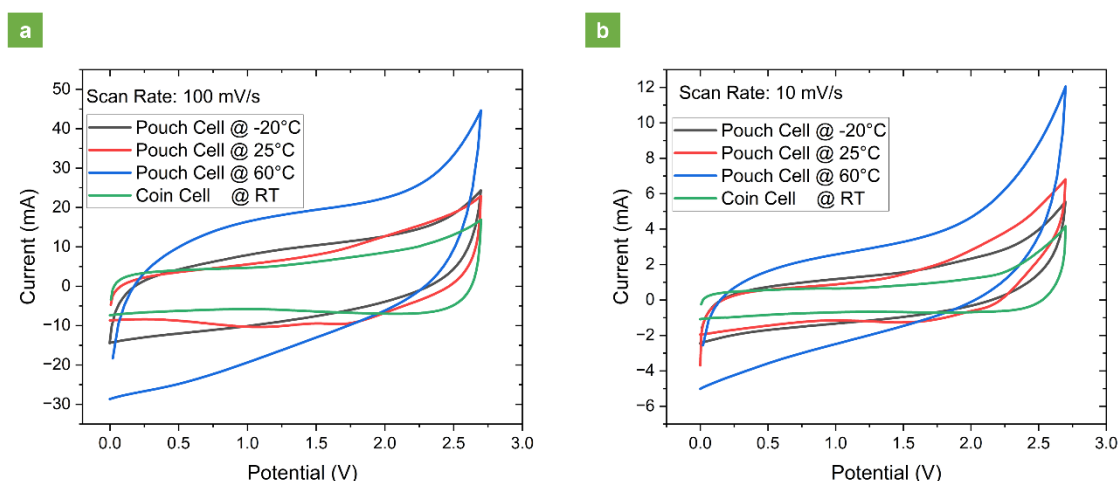


Figure 4-8: CV curves for pouch and coin cell at scan rates a) 100 mV/s ; and b) 10 mV/s

The voltammograms shown in Figure 4-8 are close to rectangular shape showing cyclic behaviour. However, some interesting curves can be observed for higher temperature. As the temperature is increased, pseudocapacitive behaviour at higher temperature can be witnessed from the curve. At 100 mV/s and 10 mV/s scan rates the pouch cell was stable and reversible at all three different temperatures, but some redox peak can be observed, especially for the $60\text{ }^{\circ}\text{C}$ measurement. The redox peaks are due to the Faradaic reactions that is happening inside the cell. There are few probable reasons for this enhanced pseudocapacitive behaviour at high temperature. As mentioned previously, organic

electrolyte (DMP-BF₄) was used for this experiment which has high stability and higher decomposition potential. Although this experiment was carried out within the safe decomposition limit (in terms of potential window and temperature⁸), at higher temperature the cell might experience vapor pressure due to some partial evaporation of the electrolyte inside the cell. This shift inside the cell might result in some change in the surface of the electrode and eventually causing physisorption of the electrolyte ions. Subsequently, there is a rise in the Faradaic current which then leads to the higher capacitance [60]. Also, as the temperature increases, the diffusion rate of the ions into the pores of the CNTs electrodes is increased which results in the increment of the effective SSA, and thus contributing to a higher capacitance [61].

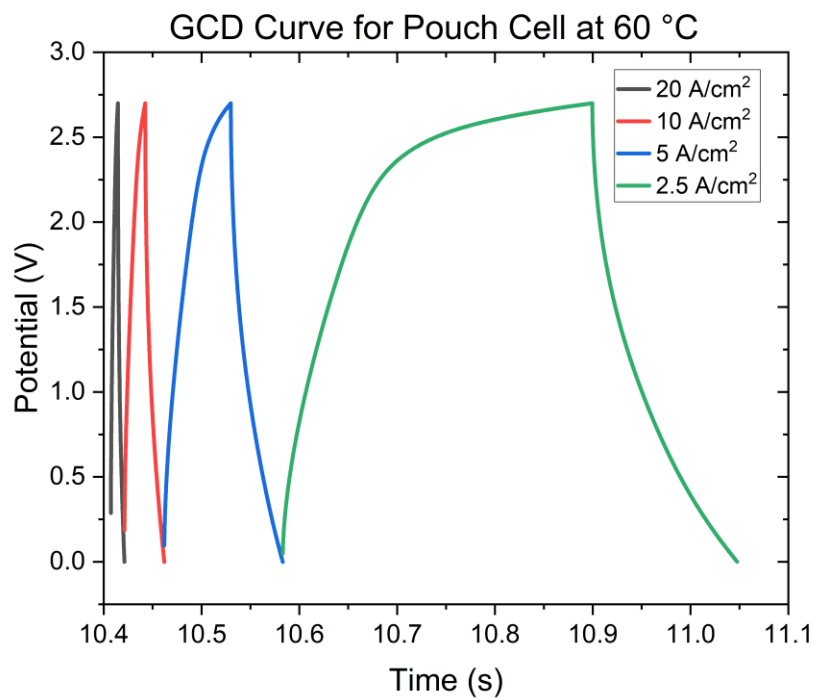


Figure 4-9: Galvanostatic charge-discharge plot for pouch cell at 60 °C for different current densities

Galvanostatic charge-discharge plots are shown in Figure 4-9 for pouch cell tested at 60 °C. Current densities of 20 A/cm², 10 A/cm², 5 A/cm², and 2.5 A/cm² were applied over a potential of 2.7 V. GCD curves give an overview of the charge-discharge cycles of the SC. GCD curves with linear and triangular shape depict capacitive behaviour of the SC. Usually

⁸ Boiling point of the electrolyte mentioned in the datasheet: 82 °C.

at higher current densities, i.e., higher current applied per unit area of electrode, the ions from the electrolyte get less time to get infiltrated into the porous structures of the CNTs. This is normal for the porous nature of CNTs. On the other hand, at lower current densities the ions get enough time to get into all the pores that are accessible to them and more importantly, Faradaic reactions causing the ions to react and delaying the time to reach the desired potential [62]. Therefore, the charge time is prolonged that affects the shape of the curve interrupting from ideal capacitive behaviour and showing pseudocapacitance as mentioned earlier. In addition, GCD curves usually have a voltage drop, known as IR drop, at the peak of the potential before the discharging starts. This portrays the ESR of the electrode or the device and can be used to determine the parameter. Same as CV, long term cycling can be done with GCD to determine the cyclic stability of the SC. GCD can also be utilised to find several other parameters.

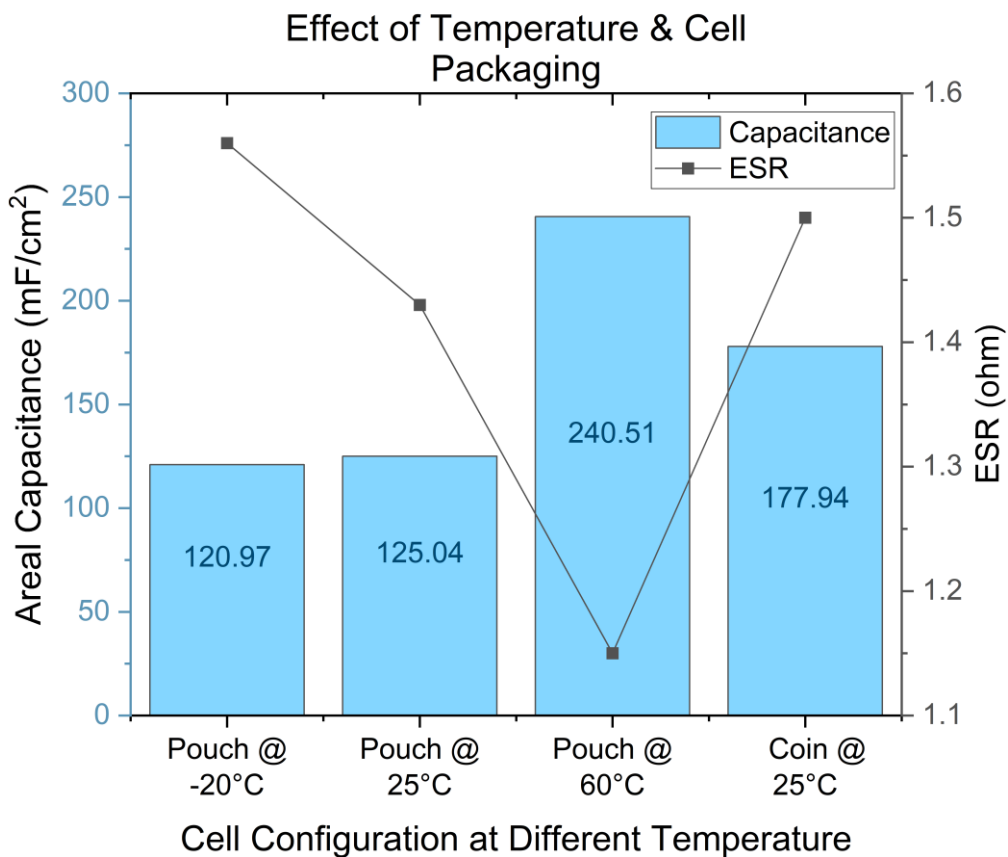


Figure 4-10: Areal capacitance and ESR at different temperature and cell configuration

As can be seen from the bar-chart-graph in Figure 4-10, the specific capacitance is proportional to the temperature, which is in agreement with the above discussion. The

highest capacitance was 240.51 mF/cm² for pouch at 60°C and with the lowest ESR of only 1.15 Ω. The CV data of 10 mV/s was used to calculate the capacitances shown.

In terms of the ESR, the higher resistance value at -20 °C can be due to the increased viscosity and lower ionic conductivity of the electrolyte. On the other hand, high temperature facilitates the accumulation of electrolyte ions and charge transfer at the electrolyte-electrode boundary, leading to a lower internal resistance [61] as shown in the graph.

Now, to evaluate the packaging configuration pouch cell and coin cell tested at 25 °C were taken into consideration. The data from coin cell and pouch cell are tested with the same physical conditions- same temperature, same CNTs electrode (CNT-SP2) from same sample, same electrolyte, separator, substrate etc. Only the package configuration is different. So, data from pouch cell and coin cell can be compared as listed in Table 2.

Table 2: Comparison of pouch cell and coin cell in terms of capacitance, energy density, power density, ESR and time constant

<i>Cell Configuration</i>	<i>Specific Capacitance of Device (mF/cm²)</i>	<i>Gravimetric Capacitance of Device (F/g)</i>	<i>Power Density of Device (W/kg)</i>	<i>Energy Density of Device (Wh/kg)</i>	<i>ESR (ohm)</i>	<i>Time Constant, τ (ms)</i>
Pouch @ 25 °C	62.52	11.14	444.1	11.28	1.43	89.4
Coin @ 25 °C	88.97	15.85	326.2	16.06	1.50	133.5

From the data, it is observed that the pouch cell has less specific capacitance compared to the coin cell, and this effects its energy density as well. Because energy density is related to the capacitance of the device. Here, if a closer look at the ESR is put then it can be seen that when the device resistance is lower it leads to high power density and much less time constant. This gives an indication of the power and charging capability of the device. Time constant is a measure of how fast a SC device response in terms of charging and discharging. For a RC circuit model time constant, τ, represents the voltage change of the device by 36.8% during charging-discharging process [46]. For both pouch cell and coin cell the time constants are in millisecond which is really good for application where instant power for only a short time is necessary such as smart wearables and implantable

bioelectronics. Here, comparison of energy density would not be effective because larger modules of SCs can do that job, but for high power application in small devices these compact packaging techniques are useful.

For the ESR another point to note is that, for pouch cells the tabs are ultrasonically welded with the current collector which might increase the conductivity and cause the lower ESR. But then again, the tab itself is made to connect to the outside of the pouch cell so it might have some internal resistance of itself, so there is a trade-off. Same thing goes for the coin cell as well there are many parts inside the coin cells that might increase the internal resistance and causing a little higher value.

It is worth mentioning that coin cell is known for its mechanical and chemical stability but for pouch cell it is always not the case and that is reflected in the data. Laboratory scale pouch cells do not always have the strong contact within the cell. The contact between the electrode-separator depends on the amount of vacuum when the final sealing is done. Also, for pouch cell there is no solid pressure on the electrodes, like coin cell, which might lead to lower capacitance. Whereas, for coin cells the contact between the electrodes through the separator are much prominent and might be the reason the higher capacitance values. An effort was made by placing plates on both sides of the pouch cell, shown in Annexes. Nonetheless, it is important to note that the difference is not significant when it comes to laboratory scale test. So, depending on the application both coin cell and pouch cells are good candidates for numerous applications in the energy storage technology. Further investigations on other parameters of both the package configurations can be done to provide a comprehensive study.

4.2.4 Effect of Crimp Pressure on Coin Cell SC Performance

To investigate the effect of crimp pressure, pressure that is exerted for coin cell assembly, on the performance of the coin cell type SC electrodes from sample CNT-SP2 was used to make one coin cell. After each time a pressure was applied, electrochemical measurements were conducted. During the crimp it was made sure that the cells are not deformed, thus this test was done after few trials with some other samples. Calculated data are from CV at a scan rate of 100 mV/s.

CV and Nyquist impedance plot from that study is presented in Figure 4-11 and Figure 4-12. From the plot it can be vividly observed that as the pressure is increased, the capacitance

increases proportionately. However, there is a saturation in the 1.0 T-1.4 T region and the specific capacitance tend to be reaching a maximum point 73.2 mF/cm². Still, the ESR shows the lowest value at 1.4 T (see Figure 4-12). The capacitance results can be explained in the way that as the pressure was increased the contact between the electrode, separator and current collector was enhanced, thus leading to proper electrical contact. This caused an increased force on the active materials of the electrodes that contributed to the enhanced exchange of the electrolyte ions through the separator and resulting in superior higher capacitance. Generally, with increase in pressure of a cell, the cyclic performance also enhances [63].

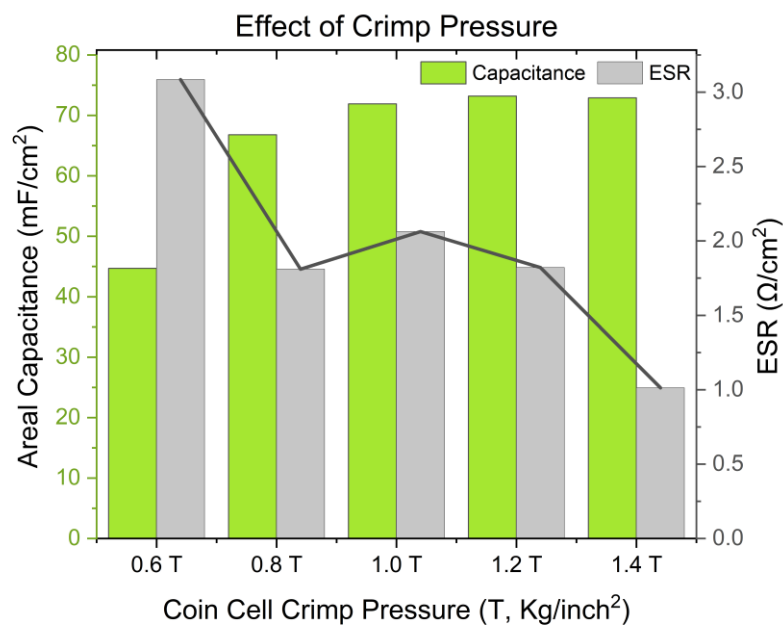


Figure 4-11: Bar chart showing the effect of coin cell crimp pressure on capacitance & ESR.

ESR is usually lower if the contact between the current collector and the cell casing is more because of increased conductivity. So, the resistance decreases if the electrical conductivity is higher. The coin cell casing is made of steel, so if the coin cells are coated with a thin layer of Au, which has high electrical conductivity and less resistivity, the ESR might be reduced. This can be implemented for future study.

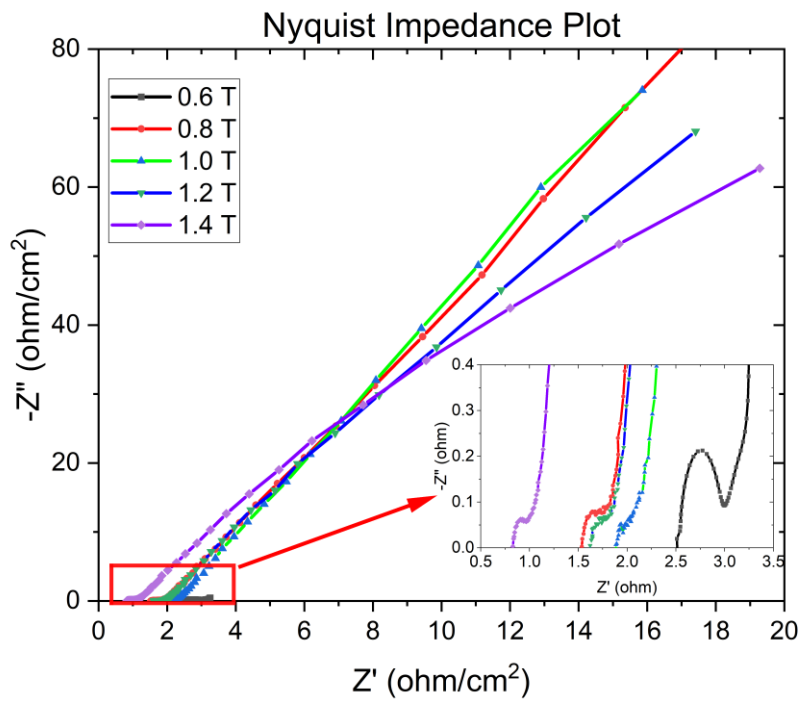


Figure 4-12: Nyquist impedance plot at different crimp pressure

Table 3: Effect of coin cell crimp pressure on capacitance, power density, energy density and ESR

Pressure (T, Kg/inch ²)	Specific Capacitance of Electrode (mF/cm ²)	Gravimetric Capacitance of Device (F/g)	Power Density of Device (W/kg)	Energy Density of Device (Wh/kg)	ESR (ohm)
0.6 T	44.7	7.96	167.0	4.03	2.93
0.8 T	66.8	11.9	284.5	6.03	1.72
1.0 T	71.9	12.8	249.7	6.49	1.96
1.2 T	73.2	13.1	282.9	6.61	1.73
1.4 T	72.9	13.0	508.7	6.58	0.96

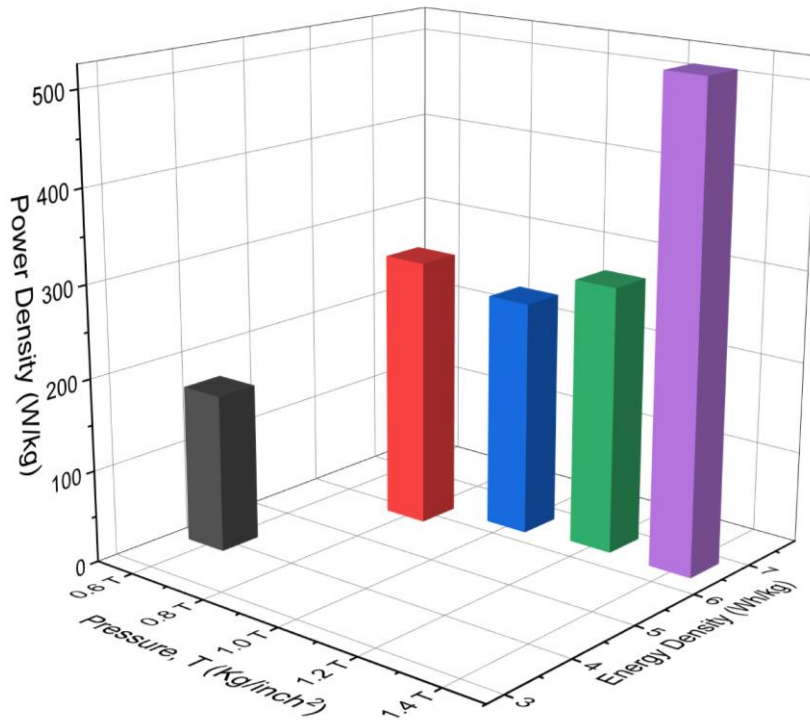


Figure 4-13: Bar chart showing the energy and power density at different crimp pressure

Table 3 and Figure 4-13 provide a broad overview of the data for specific capacitance, gravimetric capacitance, power density, energy density and ESR for different crimp pressure on coin cell. CV plots for this crimp pressure study are presented in the Annexes. As energy density is directly related to the potential window and capacitance, it follows the same trend as of the capacitance (see Eq. (14)). On the other hand, power density is directly related to potential but inversely related to the ESR values. So, higher power density is achieved at lower ESR. Therefore, it can be inferred that for applications where higher capacitance and moderate ESR are preferred, for those applications 1.2 T pressure can be a suitable crimp pressure for CR2032 (all the parameters mentioned in experimental setup) type coin cell that uses Al-CNTs electrodes synthesised by the APCVD process. For applications with the need for higher power and faster response time, 1.4 T crimp pressure is appropriate. Improvement of the capacitance can be done by more cycling of the cell. Further research can be conducted by implementing another spacer inside the coin cell which might increase the contact and pressure inside. Moreover, research can be performed to integrate the coin cell into an electronic circuit system and then evaluating the circuit performance. This will give more insight on the actual performance of the SC cell under a real-life condition.

4.2.5 Cyclic Stability of Supercapacitor

One of the important parameters for SCs is its cyclic stability. SCs usually have a reputation of longer lifetime than that of battery owing to its very good cycling stability. Commercial SCs can have lifetime of even up to million cycles. Carbon electrodes usually have a very high cycling stability [9]. In the laboratory scale SCs are usually tested for 1000-10,000 cycles or even more. One cycle means that the SCs will charge and discharge one cycle.

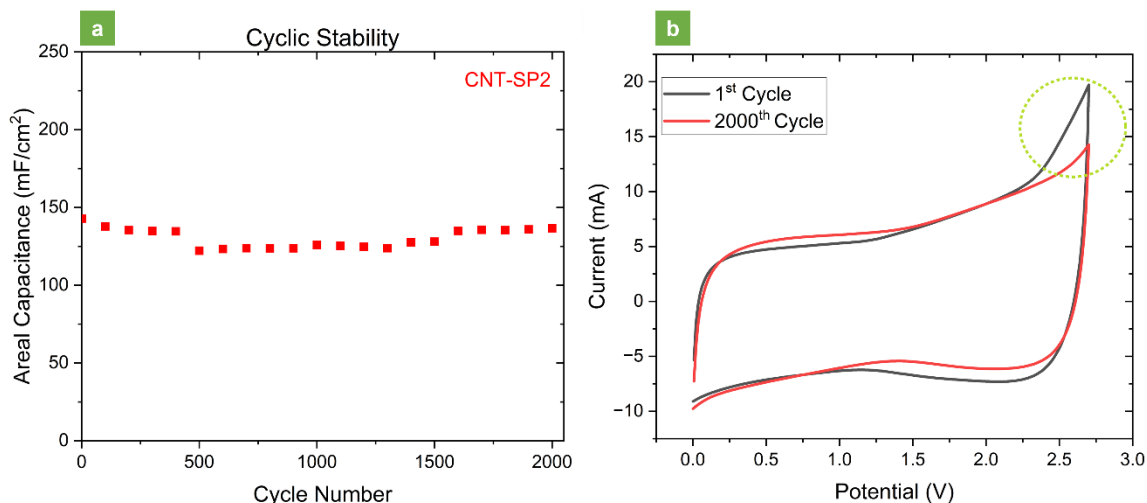


Figure 4-14: Graphs showing a) the cyclic stability and b) variation from 1st and 2000th cycle for CNT-SP2 coin cell

The graphs from Figure 4-14 show the cyclic stability performance for CNT-SP2 coin cell. The SC was cycled by running CV for 2000 cycles at a scan rate of 100 mV/s. From Figure 4-14 a) the cycling performance can be seen from 1st cycle to the last. Initially for the first hundred cycles the device was trying to stabilise in terms of the exchange of ions so there is a slight deviation in the capacitance retention. But as the device has been stabilising, the capacitive retention is much stable and it continues throughout as a straight line which can be observed from the graph. This can also be seen from Figure 4-14 b, where the initial cycle shows a slight peak in the curve and after 2000th cycle that peak is stabilised. This peak can contribute to a deviation in the capacitance after the cycling. So, from the cyclic stability test the initial and last cycle capacitance values are compared to evaluate the performance and durability of the device. The capacitance changed from 143 mF/cm² to 137 mF/cm² which shows ~96% retention in the capacitance of the device, which is similar to other studies of similar SCs [64]. This indicates the superior cycling stability and efficiency of the CNTs based SCs. However, the reason for the decreased capacitance is

due to higher number of cycling, there might be deterioration of the electrode and corrosion of the cell. So, the intercalation and deintercalation of the electrolyte ions to balance the overall charge imposes mechanical stress to the CNT electrodes [45]. Therefore, a repeated charge-discharging cycles will lead to capacitance degradation and also increase the ESR of the cell.

4.3 Proposed Chip Type Surface Mount Packaging Solution

To implement the idea of the chip type SC that can be integrated into smaller and thinner electronic components/device as a surface mount packaging, several approaches were initiated. Here, the main advantages of this chip-type SC are its lower device area, lower volume, high capacity, good charge voltage that is compatible for electronics, quick charge behaviour and many more useful properties mentioned previously.

4.3.1 Proposed Packaging Solution

To begin with, a schematic of the design is shown in Figure 4-15. A similar drawing with proper scaling is made in SolidWorks as a 3-D design for getting a better understanding of the device and its components. Length, width and height are in the ratio 3:2:1.

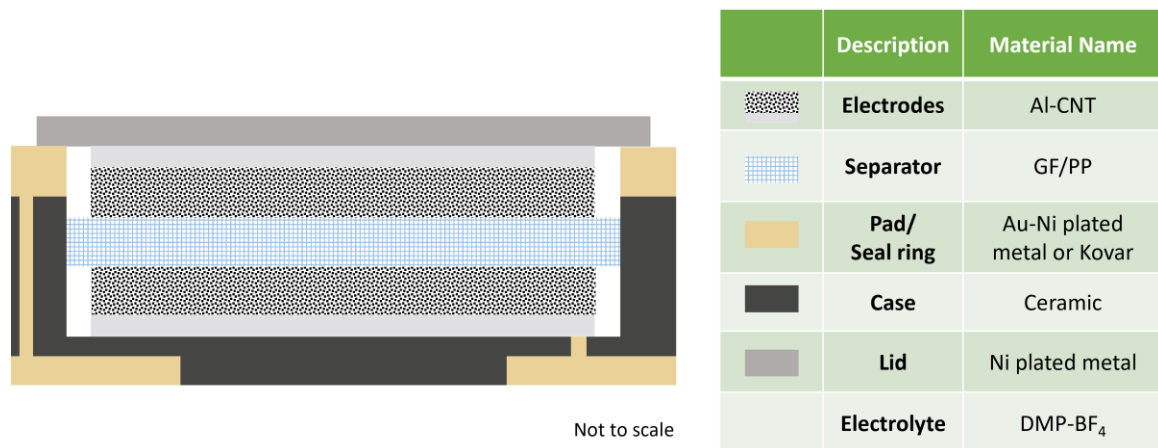


Figure 4-15: Cross-sectional schematic of the proposed chip type SC

Separator can be of glass fibre (GF) or polypropylene type that are usually used for SCs. Electrolyte for the any SC is important for the operating voltage, so organic electrolyte DMP-BF₄ is chosen similar as coin and pouch cell. The Al-CNT electrodes and separators are placed inside the package like that of a coin cell. As the cell is symmetrical, both the anodes and cathodes are the same. All these materials were already discussed in the previous

chapters. So, when it comes to the chip type SC packaging the materials are of great concern to make it a compact and robust device. In this regard, few of the material choices are listed and labelled both in Figure 4-15 and Figure 4-16.

For this type of SC, compact packaging is crucial. Hermetic sealing⁹ or encapsulation is important to provide airtightness and preventing any leakage. Ceramic is chosen as the outer package or the encapsulation of the whole device owing to its several advantages to for the electronics application such as ability to withstand high temperature, good thermal distribution and transportation, does not have any organic content so prevents decomposition like polymers or epoxies, does not absorb moisture, does not need adhesion layer etc [65]. All these properties are essential for a SC device and thus it is the main choice for the outer casing/package.

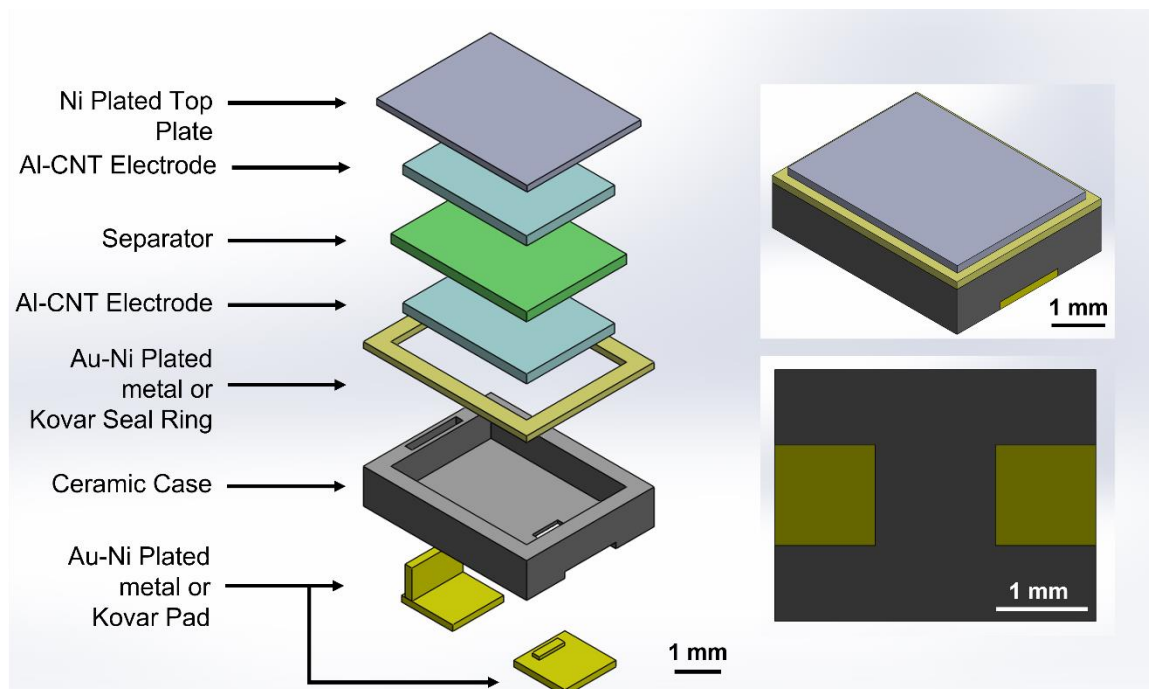


Figure 4-16: Detailed 3-D diagram and overview of the proposed chip type SC

For the terminal pads and seal ring, Kovar¹⁰ is good choice because of its ability to handle heat, good conductivity, less electrical resistivity and it is a common choice for hermetic sealing with ceramic [66]. However, to make the package more conductive and less resistive to decrease the ESR, gold-Nickel (Au-Ni) plated metal can be even a better choice.

⁹ Making airtight and leak proof.

¹⁰ Fe-Ni-Co alloy

Because the electrical resistivity of Au is around $0.022 \mu\Omega.m$ [67] whereas for the Kovar it is $0.49 \mu\Omega.m$ [66]. So, the choice for this depends on the application as well as the cost. Next, Ni plated metal is chosen for the top plate. Ni acts as a good electrical conductor both in terms of properties and price. The pads can be connected industrially by sintering. For the sealing, the Ni top plate can be either laser welded or seam sealed, the former being the more industrially viable choice for its efficiency.

Now, to understand how the electrical connection is made within the package Figure 4-15 can be observed thoroughly. The Al-CNT electrodes already have the current collectors itself so they do not need extra binders or materials for electrical connections. As for the ceramic, it is not a conductor so electrical connections have to be made with the top and bottom current collector to make a proper electrical circuit connection. Ceramic can be drilled industrially on both sides of the casing to make connections with the pads and the current collector. In this way, the top current collector is connected with one pad and the bottom current collector is connected with the other. More images are provided in the Annexes for better understanding. These chip type SCs are robust and useful in the small electronics and can have numerous application benefits owing to its miniature size, higher capacity, lower internal resistance, higher power delivering capability, less volume, good compatibility with ICs and sensors etc. Thus, more research needs to be done to implement and optimise the parameters of the chip-type SCs for usage as a product.

To implement this idea into reality, an effort for lab scale prototype was made, discussed in the next sub-section.

4.3.2 Laboratory Scale Approach

A laboratory scale version of the same design mentioned above was attempted. The main concept of the design was to make it surface mount packaging device, similar to the chip-type SC. Figure 4-17 shows a schematic of the laboratory version of chip type SC.

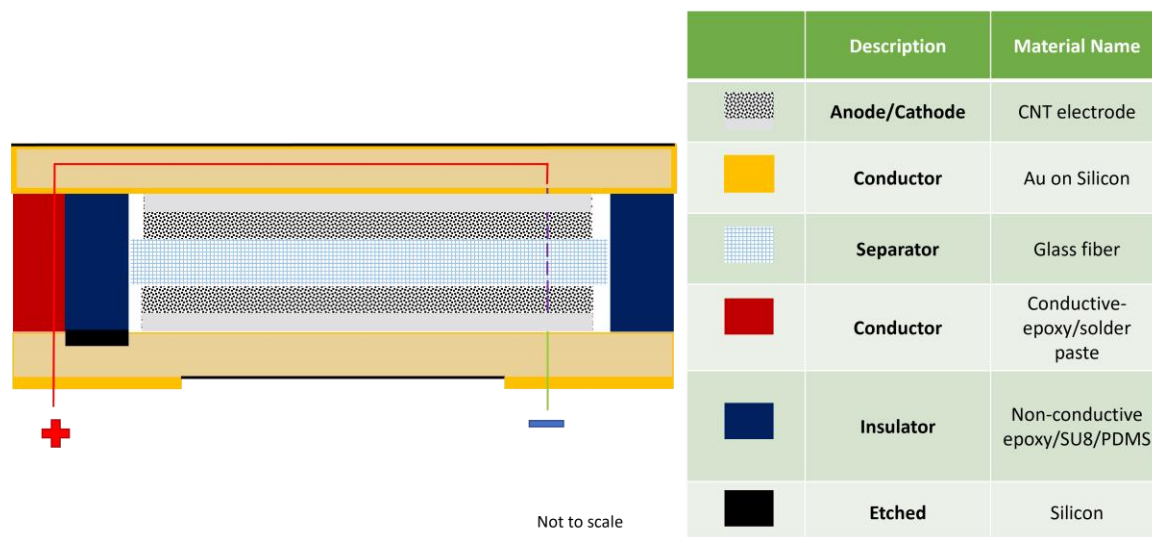


Figure 4-17: Schematic of laboratory version of chip type SC

The main idea is similar to the earlier design, but the materials were adapted according to the resources available in the laboratory. Electrodes and separators are of the same materials. Ceramic was replaced with two Si wafer deposited with Au for top and bottom plates. Thermal evaporation was used for the deposition of Au. To make things easier to handle, both sides of the Si wafers were deposited with 200 nm of Au, serving as the conductor and connector. To separate the electrodes and also the electrical connection to avoid short circuit, some parts of the Au were etched with gold etchant as shown with black line in the diagram. For supporting the top and bottom structure, insulator (epoxy), labelled as blue blocks, was placed in between the two Si wafer acting as top and bottom plates. Before they were placed, on the left side some part of the gold were also etched so as to avoid short circuit. Top and bottom parts are electrically connected with conductive silver (Ag) paste. The terminals pads were Au deposited on the back of the bottom Si wafer. The center part was etched to disconnect it from another pad. Thus, an electrical circuit is made with proper connections. Figure 4-18 shows the attempted approach with Au deposited on Si wafer.

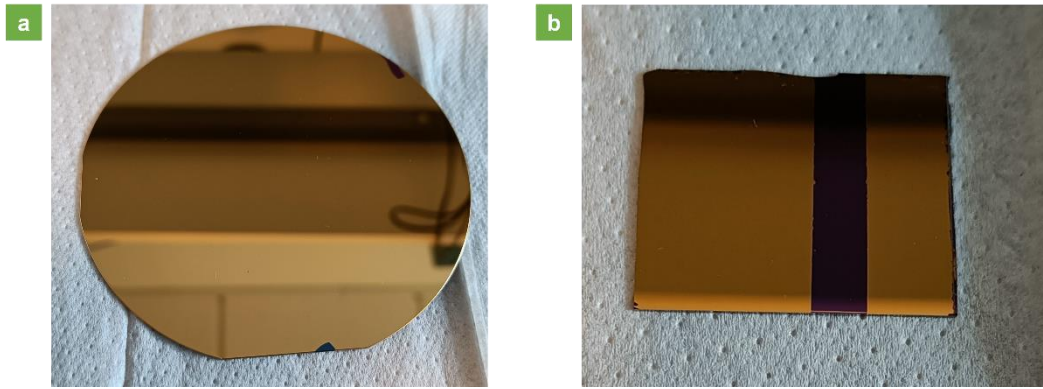


Figure 4-18: Attempted lab scale version of chip type SC with a) Au deposited on Si wafer and b) partly etched Si wafer for prototype

The intended endeavor encountered challenges primarily attributable to the necessity of achieving hermetic sealing. Regrettably, successful airtight sealing of the package could not be accomplished. The utilization of an organic electrolyte in the studied SCs necessitated the execution of the packaging procedure within a glovebox, further complicating the sealing process. Despite making various alternative design attempts, the feasibility of implementing the proposed packaging technique at a laboratory scale remained elusive. One more approach that was attempted is shown in the Annexes.

Overall, chip type SCs have immense potential for incorporating into ICs, sensors, wearables, battery backup, memory backup, and many more applications. To keep that in mind, this relatively new research field needs to be explored by the research community to maximise its potential. Although there are challenges in this field, especially for academic research, but with every challenges overcome innovation is inevitable.

4.4 State-of-the-Art Areal Capacitance with Coin Cell

Supercapacitor

This study investigated the compact packaging of SCs and tested their electrochemical characterisations to evaluate the performance. Capacitance results in terms of mF/cm^2 or F/g were calculated. Initially, when the three electrode tests were conducted, the actual device capacitance values needed to be investigated. So, packaging was done to study the capacitance when the SC is in the form of a device. Most of the packaging were done with

coin cell as this is the feasible procedure in a laboratory scale and also due to sufficient resources availability for coin cell. As for the pouch cell the assembly, packaging and tests were done at a different research facility. CNT-SP3 sample was used for the coin cell package.

Packages were optimised (such as pressure, electrolyte volume etc) to maximise the device performance. Among the different coin cells packaged and tested for evaluation, the capacitance varied from 20 mF/cm² -800 mF/cm². After optimisation of the compact packaging of coin cells, an excellent performance of the device capacitance was achieved. Figure 4-19 shows the CV curves from coin cell electrochemical characterisations of CNT-SP3 sample. The capacitance values at 100 mV/s, 50 mV/s and 5 mV/s were found to be 698 mF/cm², 930 mF/cm² and 1298 mF/cm², respectively and in terms of the gravimetric capacitance the calculated values were 45 F/g, 58 F/g and 81 F/g. These results show state-of-the-art performance of SCs based on CNTs. Here it is important to note that the capacitances can be calculated both as the electrode capacitance and device capacitance for a coin cell. When it comes to energy density and power density calculation of the device capacitance is used as it shows the capability of the overall device.

The results from the ESR also shows less resistance values for such high capacitance device. ESR value was found to be 3.6 ohm and for this test, the Nyquist impedance (see Figure 4-20) plot was curve fitted with Zfit analysis tool to find the parameters of an equivalent circuit. As mentioned in the background studies, Randles circuit is commonly used to present the different resistance natures of a SC represented by equivalent circuit. From Figure 4-20 b and c it can be observed that internal resistance, R_s , is 3.26 ohm and the charge-transfer resistance, R_{CT} , is 0.79 ohm.

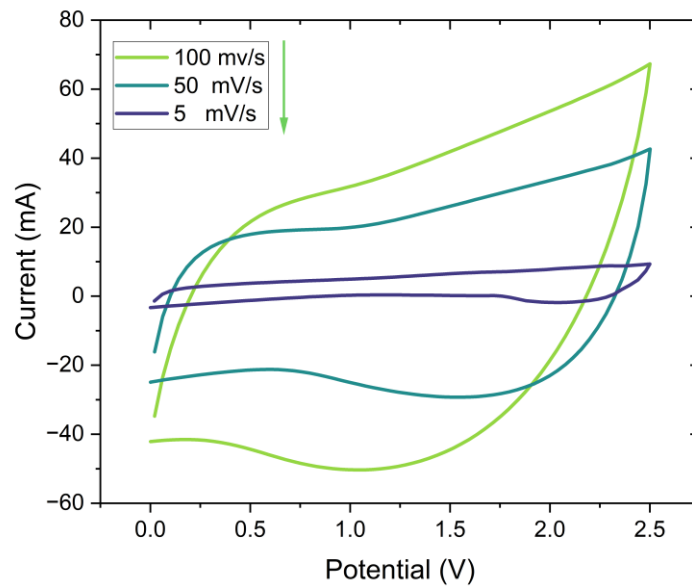


Figure 4-19: CV curve for CNT-SP3 coin cell at different scan rates

This is in agreement with the impedance plot, because for an ideal capacitor the curve would have been a semicircle and then a vertical line in the real impedance axis. But for this SC there are some diffusion and charge transfer resistance present due to the non-absorption of redox species onto the CNT electrode surface, charge depletion at the electrode interface and mass transfer diffusion (Warburg element) in the cell that are represented by R_{CT} , C_{DL} and W_0 , respectively. These elements are contributed by several factors like the material properties, electrolyte, separators and packaging techniques adopted. Post processing of CNTs electrodes before the packaging can help to improve the ESR performance. Also, using high conductivity electrolyte can play a role in the improvement.

Coming back to the performance of the CNT-SP3 coin cell, power density, energy density and time constants are calculated to give an overview of the superior performance of the device, tabulated in Table 4. From the data in the table, the gravimetric capacitance is 40.5 F/g and the power density and energy density are 129.5 W/kg and 35.2 Wh/kg, respectively.

A comparative analysis with similar SC in advanced laboratories is made in the next section.

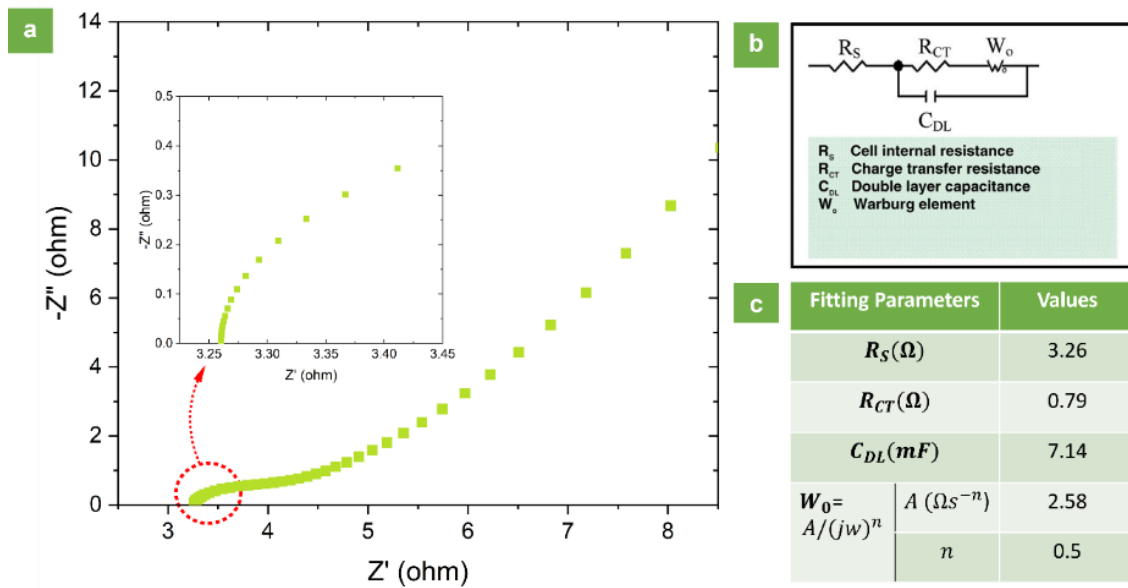


Figure 4-20: Electrochemical impedance spectroscopy for CNT-SP3 coin cell showing a) Nyquist impedance plot; b) representation of Randle equivalent circuit with parameters; and c) circuit parameters found from fitting analysis

Table 4: Calculated parameters for the high performance CNT-SP3 coin cell

Item	Areal Capacitance of Electrode (mF/cm ²)	Gravimetric Capacitance of Device (F/g)	Power Density of Device (W/kg)	Energy Density of Device (Wh/kg)	Time Constant, τ (s)	ESR (ohm)
Coin Cell CNT-SP3	1298	40.5	129.5	35.2	2.12	3.26

4.4.1 Comparison With Some Advanced Laboratory Scale SC

A comparison is made with the similar Cs in the academic research arena. As in different research studies some parameters or calculations are not adopted, it was quite challenging to gather the data from different references. In most of the research capacitance is calculated in terms of gravimetric capacitance. Still an effort has been made to list down the contemporary data to compare the results from this work.

To make the comparison homogeneous, the energy and power density were calculated as $\mu\text{Wh}/\text{cm}^2$ and $\mu\text{W}/\text{cm}^2$, respectively.

Table 5: Comparison of supercapacitor performance data from literature

	<i>Areal Capacitance (mF/cm²)</i>	<i>Power Density (μW/cm²)</i>	<i>Energy Density (μWh/cm²)</i>	<i>References</i>
CN/CNT	110	3.6	16	[68]
CC-CF	270	418.48	4.56	[69]
CNT/PC	365	2.98	10.5	[70]
FC-CNT/MnO	742	5500	51.5	[51]
Al-CNT-SP3	1298	504500	1126.7	This work
CDCA	1618	1800	289	[71]

SCs based on CNTs, carbon fibre, carbon cloth, and carbon aerogels from literature sources are listed in Table 5. From the data, it can be observed that there is a variation when it comes to the areal capacitance. Most literature study is based on the gravimetric capacitance. But for this study the primary focus was to look for viable options for SCs that have high areal capacitance as well as high energy and power density. Carbon-cloth-carbon-fibre, CC-CF, data was based on flexible supercapacitor which have moderate areal capacitance but very good power density of 418 μW/cm². The FC-CNT/MnO is a SC based on fullerene CNTs similar to the ones that is used in this work. This SC had a very good areal capacitance of 742 mF/cm² as well as high power and energy density. From the literature the highest areal capacitance for SC was found to be 1618 mF/cm² from carbon-derived carbon aerogels SC, which is a really good value. But this comes with a very low energy and power density. So, its application would be limited when it comes to device application. For many literature sources, the reported capacitance was based on only the electrode. Meanwhile, this study measured the areal capacitance that was 1298 mF/cm² in terms of only the electrode per sq. cm, and 649 mF/cm² when it is calculated as a device. Even then the areal capacitance, energy density and power density all these performance parameters are much higher than the literature sources. So, it can be inferred that compact devices with CNTs based electrode provide superior SC performance compared to its counterparts and have applications for a wide range of applications. This means that these devices can be employed in small electronics systems, ICs, chips, sensors, smart fingerprint cards, smart pen, smart wearables and many more applications. Thus, it is important to realise the

importance of compact packaging of CNTs based SCs to unlock the huge potential in the energy storage technology.

5 Conclusion and Future Work

In this thesis, the need for compact packaging of supercapacitors was addressed, considering the increasing demand for portable and integrated energy storage solutions. The objectives and research motivations were identified, focusing on the exploration of development of compact packaging techniques for supercapacitors using carbon nanotubes (CNTs) as electrode materials.

The thesis provided a comprehensive background study on supercapacitors as energy storage devices, highlighting their unique properties and advantages. The utilization of CNTs as electrode materials was investigated, emphasizing their high surface area, conductivity, and electrochemical performance. Compact packaging techniques for supercapacitors were explored, recognizing their significance in enhancing the overall performance, reliability, and integration of these devices into various applications.

The results and discussions section presented the morphology and analysis of CNT electrodes, providing insights into their structural properties and performance characteristics. The effects of physical and test parameters on supercapacitor performance were examined, highlighting the factors influencing capacitance, energy density, and power density. The results revealed that higher mass loading of active material usually leads to higher capacitance and also the electrode can have a significant influence on the result. From the analysis of the results, it was found that scan rate for CV influences the capacitance, at higher scan rate the capacitor tends to decrease due to less infiltration of electrolyte ions onto electrode surface.

The effect of different temperature conditions for pouch cell showed that at higher temperature, the capacitance of the supercapacitor device increases where the ESR value decreases owing to greater ion exchange at higher temperature. The opposite is true for cold temperature.

Effect of crimping pressure of coin cell was thoroughly studied and it was observed that at greater crimping pressure the capacitance, energy density and power density increase but there is a saturation. For the highest crimp pressure, highest power density of 509 W/kg and the lowest ESR of 0.96 ohm was found. This reveals the ability of the device for high power application. Cyclic stability of SC ensured the high and stable performance of the coin cell SC with capacitive retention of ~96%.

Additionally, a proposed chip-type surface mount packaging solution was presented, offering a promising approach for compact and integrated supercapacitor designs for portable and miniature electronic applications requiring high power and fast charging ability. Furthermore, the state-of-the-art areal capacitance with coin cell supercapacitors was found to be 1298 mF/cm^2 , showcasing the advancements in supercapacitor technology.

In conclusion, this thesis contributed to the understanding and advancement of supercapacitor technology, particularly in the areas of compact packaging techniques and performance evaluation. Despite the limited resources and challenges faced during the research, valuable insights were gained, highlighting the potential and challenges associated with the compact packaging of supercapacitors based on CNTs. The findings of this study open new avenues for further research and development in the field of energy storage technology, paving the way for future innovations in portable electronics, power management systems, and other applications that require efficient energy storage solutions.

References

- [1] Y. M. Volkovich, "Electrochemical Supercapacitors (a Review)," *Russ. J. Electrochem.* 2021 574, vol. 57, no. 4, pp. 311–347, May 2021, doi: 10.1134/S1023193521040108.
- [2] "超级电容器 (EDLC) - [烯晶碳能 — 中国高品质法拉电容器领创者]." http://www.gmccchina.com/product/product_15_1.html (accessed Jun. 12, 2023).
- [3] Tasfia Nowshin Farook, "Optimized growth of iCL-CNT on a microstructured Al substrate for high energy density supercapacitors," University of South-Eastern Norway, 2023.
- [4] "Supercapacitors Market Size, Trends, Growth, Forecast, 2030." <https://www.astuteanalytica.com/industry-report/supercapacitors-market> (accessed Jun. 30, 2023).
- [5] E. P. Dana POPP, "Making batteries more sustainable, more durable and better-performing," 2023. [Online]. Available: <https://www.europarl.europa.eu/news/en/press-room/20230609IPR96210/making-batteries-more-sustainable-more-durable-and-better-performing>
- [6] B. E. Conway, "Electrochemical Supercapacitors," *Electrochem. Supercapacitors*, 1999, doi: 10.1007/978-1-4757-3058-6.
- [7] P. Sinha and K. K. Kar, "Introduction to supercapacitors," *Springer Ser. Mater. Sci.*, vol. 302, pp. 1–28, 2020, doi: 10.1007/978-3-030-52359-6_1/FIGURES/7.
- [8] BioLogic, "Supercapacitors and insertion batteries: what are the differences?" <https://www.biologic.net/topics/supercapacitors-insertion-batteries-differences/> (accessed Jun. 10, 2023).
- [9] C. Zhong, Y. Deng, W. Hu, J. Qiao, L. Zhang, and J. Zhang, "A review of electrolyte materials and compositions for electrochemical supercapacitors," *Chem. Soc. Rev.*, vol. 44, no. 21, pp. 7484–7539, Oct. 2015, doi: 10.1039/C5CS00303B.
- [10] P. Forouzandeh, V. Kumaravel, and S. C. Pillai, "Electrode Materials for Supercapacitors: A Review of Recent Advances," *Catal. 2020, Vol. 10, Page 969*, vol. 10, no. 9, p. 969, Aug. 2020, doi: 10.3390/CATAL10090969.

- [11] B. De, S. Banerjee, K. D. Verma, T. Pal, P. K. Manna, and K. K. Kar, "Carbon nanotube as electrode materials for supercapacitors," *Springer Ser. Mater. Sci.*, vol. 302, pp. 229–243, 2020, doi: 10.1007/978-3-030-52359-6_9/FIGURES/11.
- [12] V. S. Bagotsky, A. M. Skundin, A. M. Skundin, and Y. M. Volkovich, "Electrochemical Power Sources: Batteries, Fuel Cells, and Supercapacitors," 2015, [Online]. Available: <https://scholar.google.com/scholar?q=Electrochemical Power Sources: Batteries, Fuel Cells, and Supercapacitors>
- [13] X. Huang, "Separator technologies for lithium-ion batteries," *J. Solid State Electrochem.*, vol. 15, no. 4, pp. 649–662, 2011, doi: 10.1007/s10008-010-1264-9.
- [14] M.-N. G. & C. KG, "Filtration downloads | MACHEREY-NAGEL." <https://www.mn-net.com/Filtration-downloads> (accessed Jun. 21, 2023).
- [15] P. Simon and Y. Gogotsi, "Materials for electrochemical capacitors," *Nat. Mater.*, vol. 7, no. 11, pp. 845–854, 2008, doi: 10.1038/nmat2297.
- [16] K. D. Verma, P. Sinha, S. Banerjee, and K. K. Kar, "Characteristics of Current Collector Materials for Supercapacitors BT - Handbook of Nanocomposite Supercapacitor Materials I: Characteristics," K. K. Kar, Ed. Cham: Springer International Publishing, 2020, pp. 327–340. doi: 10.1007/978-3-030-43009-2_12.
- [17] G. Wang, L. Zhang, and J. Zhang, "A review of electrode materials for electrochemical supercapacitors," *Chem. Soc. Rev.*, vol. 41, no. 2, pp. 797–828, Jan. 2012, doi: 10.1039/C1CS15060J.
- [18] T. Chen and L. Dai, "Carbon nanomaterials for high-performance supercapacitors," *Mater. Today*, vol. 16, no. 7–8, pp. 272–280, Jul. 2013, doi: 10.1016/J.MATTOD.2013.07.002.
- [19] M. Vorotyntsev, "Modern Aspects of Electrochemistry," *New York Plenum*, vol. 17, p. 131, 1986.
- [20] J. Kong, H. T. Soh, A. M. Cassell, C. F. Quate, and H. Dai, "Synthesis of individual single-walled carbon nanotubes on patterned silicon wafers," *Nat.* 1998 3956705, vol. 395, no. 6705, pp. 878–881, Oct. 1998, doi: 10.1038/27632.
- [21] M. Ahmad and S. R. P. Silva, "Low temperature growth of carbon nanotubes – A review," *Carbon N. Y.*, vol. 158, pp. 24–44, Mar. 2020, doi: 10.1016/J.CARBON.2019.11.061.
- [22] LU Pai ; Chen Xuyuan, "Deposited carbon film on etched silicon for on-chip

- supercapacitor,” US 2020/0013560 A1, 2020 [Online]. Available: <https://patents.google.com/patent/EP3593371B1/en>
- [23] Q. Cheng, J. Tang, J. Ma, H. Zhang, N. Shinya, and L. C. Qin, “Graphene and carbon nanotube composite electrodes for supercapacitors with ultra-high energy density,” *Phys. Chem. Chem. Phys.*, vol. 13, no. 39, pp. 17615–17624, Sep. 2011, doi: 10.1039/C1CP21910C.
- [24] A. N. Redkin, A. A. Mitina, and E. E. Yakimov, “Simple technique of multiwalled carbon nanotubes growth on aluminum foil for supercapacitors,” *Mater. Sci. Eng. B*, vol. 272, p. 115342, 2021, doi: <https://doi.org/10.1016/j.mseb.2021.115342>.
- [25] K. DU, X. CHEN, and P. A. ØHLCKERS, “DIRECT GROWTH CROSS-LINKED CARBON NANOTUBES ON MICROSTRUCTURED METAL SUBSTRATE FOR SUPERCAPACITOR APPLICATION,” Apr. 2022.
- [26] M. Barrejón, R. Rauti, L. Ballerini, and M. Prato, “Chemically Cross-Linked Carbon Nanotube Films Engineered to Control Neuronal Signaling,” *ACS Nano*, vol. 13, no. 8, pp. 8879–8889, Aug. 2019, doi: 10.1021/acsnano.9b02429.
- [27] S. Ozden *et al.*, “Chemically interconnected light-weight 3D-carbon nanotube solid network,” *Carbon N. Y.*, vol. 119, pp. 142–149, Aug. 2017, doi: 10.1016/J.CARBON.2017.03.086.
- [28] “Technology - nanoCaps.” <https://nanocaps.no/technology/> (accessed Jun. 15, 2023).
- [29] S. Banerjee, B. De, P. Sinha, J. Cherusseri, and K. K. Kar, “Applications of supercapacitors,” *Springer Ser. Mater. Sci.*, vol. 300, pp. 341–350, 2020, doi: 10.1007/978-3-030-43009-2_13/FIGURES/8.
- [30] L. F. Aval, M. Ghoranneviss, and G. B. Pour, “High-performance supercapacitors based on the carbon nanotubes, graphene and graphite nanoparticles electrodes,” *Heliyon*, vol. 4, no. 11, p. e00862, Nov. 2018, doi: 10.1016/J.HELİYON.2018.E00862.
- [31] Y. Han *et al.*, “Review of Flexible Supercapacitors Using Carbon Nanotube-Based Electrodes,” *Appl. Sci. 2023, Vol. 13, Page 3290*, vol. 13, no. 5, p. 3290, Mar. 2023, doi: 10.3390/APP13053290.
- [32] K. M. Joseph, H. J. Kasparian, and V. Shanov, “Carbon Nanotube Fiber-Based Wearable Supercapacitors—A Review on Recent Advances,” *Energies 2022, Vol. 15, Page 6506*, vol. 15, no. 18, p. 6506, Sep. 2022, doi: 10.3390/EN15186506.

- [33] W. Lu, L. Dai, W. Lu, and L. Dai, "Carbon Nanotube Supercapacitors," *Carbon Nanotub.*, Mar. 2010, doi: 10.5772/39444.
- [34] V. V. N. Obreja, "Advance in the assembling and packaging of supercapacitor modules for higher performance," *Proc. - 2008 2nd Electron. Syst. Technol. Conf. ESTC*, pp. 771–774, 2008, doi: 10.1109/ESTC.2008.4684448.
- [35] S. Brahim, S. Zhang, and S. Maat, "High Energy Density Carbon Nanotube-Based Supercapacitors," *ECS Meet. Abstr.*, vol. MA2022-01, no. 1, p. 2, Jul. 2022, doi: 10.1149/MA2022-0112MTGABS.
- [36] I. Nam, G. P. Kim, S. Park, J. Park, N. D. Kim, and J. Yi, "Fabrication and design equation of film-type large-scale interdigitated supercapacitor chips," *Nanoscale*, vol. 4, no. 23, pp. 7350–7353, Nov. 2012, doi: 10.1039/C2NR31961F.
- [37] A. Soam, N. Arya, A. Singh, and R. Dusane, "Fabrication of silicon nanowires based on-chip micro-supercapacitor," *Chem. Phys. Lett.*, vol. 678, pp. 46–50, Jun. 2017, doi: 10.1016/J.CPLETT.2017.04.019.
- [38] H. Hu, Z. Pei, and C. Ye, "Recent advances in designing and fabrication of planar micro-supercapacitors for on-chip energy storage," *Energy Storage Mater.*, vol. 1, pp. 82–102, Nov. 2015, doi: 10.1016/J.ENSM.2015.08.005.
- [39] K. Wang *et al.*, "An All-Solid-State Flexible Micro-supercapacitor on a Chip," *Adv. Energy Mater.*, vol. 1, no. 6, pp. 1068–1072, Nov. 2011, doi: 10.1002/AENM.201100488.
- [40] "New Reflowable and Low Impedance Chip-Type Capacitor Ideal for data backup, power assist and energy harvesting | Seiko Instruments Inc." <https://www.sii.co.jp/en/news/release/2015/07/16/11183/> (accessed Jun. 16, 2023).
- [41] "Low resistance, thin, and lightweight electric double-layer capacitors (EDLC/supercapacitors) | Product Overview | Tech Library | TDK Product Center." <https://product.tdk.com/en/techlibrary/productoverview/slim-pouch-edlc.html> (accessed Jun. 15, 2023).
- [42] "Gelon Cr2032 Coin Button Cell Case with Spring and Spacer - China Cr2032 and Coin Cell Case price." <https://gelonlib.en.made-in-china.com/product/OZKAcSijQtUd/China-Gelon-Cr2032-Coin-Button-Cell-Case-with-Spring-and-Spacer.html> (accessed Jun. 16, 2023).

- [43] S. S. Karade, S. Lalwani, J. H. Eum, and H. Kim, "Coin cell fabricated symmetric supercapacitor device of two-steps synthesized V₂O₅ Nanorods," *J. Electroanal. Chem.*, vol. 864, p. 114080, May 2020, doi: 10.1016/J.JELECHEM.2020.114080.
- [44] J. W. Choi and D. Aurbach, "Promise and reality of post-lithium-ion batteries with high energy densities," *Nat. Rev. Mater.*, vol. 1, no. 4, p. 16013, 2016, doi: 10.1038/natrevmats.2016.13.
- [45] B. K. Kim, S. Sy, A. Yu, and J. Zhang, "Electrochemical Supercapacitors for Energy Storage and Conversion," *Handb. Clean Energy Syst.*, pp. 1–25, Jul. 2015, doi: 10.1002/9781118991978.HCES112.
- [46] S. Zhang, N. Pan, S. Zhang, and N. Pan, "Supercapacitors Performance Evaluation," *Adv. Energy Mater.*, vol. 5, no. 6, p. 1401401, Mar. 2015, doi: 10.1002/AENM.201401401.
- [47] F. Daneshvar, H. Chen, K. Noh, and H. J. Sue, "Critical challenges and advances in the carbon nanotube–metal interface for next-generation electronics," *Nanoscale Adv.*, vol. 3, no. 4, p. 942, Feb. 2021, doi: 10.1039/D0NA00822B.
- [48] A. G. Olabi, Q. Abbas, M. A. Abdelkareem, A. H. Alami, M. Mirzaeian, and E. T. Sayed, "Carbon-Based Materials for Supercapacitors: Recent Progress, Challenges and Barriers," *Batter. 2023, Vol. 9, Page 19*, vol. 9, no. 1, p. 19, Dec. 2022, doi: 10.3390/BATTERIES9010019.
- [49] H. S. Magar, R. Y. A. Hassan, and A. Mulchandani, "Electrochemical Impedance Spectroscopy (EIS): Principles, Construction, and Biosensing Applications," *Sensors (Basel)*, vol. 21, no. 19, Oct. 2021, doi: 10.3390/S21196578.
- [50] P. Vadhva *et al.*, "Electrochemical Impedance Spectroscopy for All-Solid-State Batteries: Theory, Methods and Future Outlook," *ChemElectroChem*, vol. 8, no. 11, pp. 1930–1947, Jun. 2021, doi: 10.1002/CELC.202100108.
- [51] P. Lu, X. Chen, P. Ohlckers, E. Halvorsen, M. Hoffmann, and L. Müller, "DRIE Si Nanowire Arrays Supported Nano-Carbon Film for Deriving High Specific Energy Supercapacitors On-Chip," *J. Phys. Conf. Ser.*, vol. 1837, no. 1, p. 012005, Mar. 2021, doi: 10.1088/1742-6596/1837/1/012005.
- [52] MTI Corporation, "Pressure Adjustable Electric Crimper for CR20XX Button Cells - MSK-160E."
<https://www.mtixtl.com/PressureAdjustableElectricCrimperforCR20XXButtonCells->

- MSK-160E.aspx (accessed Jun. 17, 2023).
- [53] V. Ghai, K. Chatterjee, and P. K. Agnihotri, "Vertically aligned carbon nanotubes-coated aluminium foil as flexible supercapacitor electrode for high power applications," *Carbon Lett.*, vol. 31, no. 3, pp. 473–481, 2021, doi: 10.1007/s42823-020-00176-4.
- [54] P. L. Taberna, P. Simon, and J. F. Fauvarque, "Electrochemical Characteristics and Impedance Spectroscopy Studies of Carbon-Carbon Supercapacitors," *J. Electrochem. Soc.*, vol. 150, no. 3, p. A292, Jan. 2003, doi: 10.1149/1.1543948/XML.
- [55] J. Sengupta and C. Jacob, "The effect of Fe and Ni catalysts on the growth of multiwalled carbon nanotubes using chemical vapor deposition," *J. Nanoparticle Res.*, vol. 12, no. 2, pp. 457–465, 2010, doi: 10.1007/s11051-009-9667-1.
- [56] H. Ahmed, "Optimized Ni Nanoparticle Deposition for iCL-CNT Growth for High Energy Density Supercapacitors," University of South-Eastern Norway, 2023.
- [57] S. Y. Moon, I. J. Kang, S. M. Kim, and W. S. Kim, "Influence of the Sulfur Content Catalyst on the Packing Density of Carbon Nanotube Forests.," *Nanomater. (Basel, Switzerland)*, vol. 9, no. 6, Jun. 2019, doi: 10.3390/nano9060889.
- [58] V. Țucureanu, A. Matei, and A. M. Avram, "FTIR Spectroscopy for Carbon Family Study," *Crit. Rev. Anal. Chem.*, vol. 46, no. 6, pp. 502–520, Nov. 2016, doi: 10.1080/10408347.2016.1157013.
- [59] L. Lyu *et al.*, "CNT/High Mass Loading MnO₂/Graphene-Grafted Carbon Cloth Electrodes for High-Energy Asymmetric Supercapacitors," *Nano-Micro Lett.*, vol. 11, no. 1, p. 88, 2019, doi: 10.1007/s40820-019-0316-7.
- [60] C. Masarapu, H. F. Zeng, K. H. Hung, and B. Wei, "Effect of Temperature on the Capacitance of Carbon Nanotube Supercapacitors," *ACS Nano*, vol. 3, no. 8, pp. 2199–2206, Aug. 2009, doi: 10.1021/nn900500n.
- [61] G. Xiong, A. Kundu, and T. S. Fisher, "Influence of Temperature on Supercapacitor Performance BT - Thermal Effects in Supercapacitors," G. Xiong, A. Kundu, and T. S. Fisher, Eds. Cham: Springer International Publishing, 2015, pp. 71–114. doi: 10.1007/978-3-319-20242-6_4.
- [62] Z. Niu *et al.*, "Compact-designed supercapacitors using free-standing single-walled carbon nanotube films," *Energy Environ. Sci.*, vol. 4, no. 4, pp. 1440–1446, Mar. 2011, doi: 10.1039/C0EE00261E.

- [63] S. Burlatsky *et al.*, “Communication—Anode-Free Lithium Metal Batteries: A Case Study of Compression Effects on Coin Cell Performance,” *J. Electrochem. Soc.*, vol. 168, no. 6, p. 060532, Jun. 2021, doi: 10.1149/1945-7111/AC0998.
- [64] M. Zhong, M. Zhang, and X. Li, “Carbon nanomaterials and their composites for supercapacitors,” *Carbon Energy*, vol. 4, no. 5, pp. 950–985, Sep. 2022, doi: 10.1002/CEY2.219.
- [65] T. Bartnitzek, T. Thelemann, S. Apel, and K.-H. Suphan, “Advantages and limitations of ceramic packaging technologies in harsh applications”.
- [66] “Kovar Tech Data.” <https://www.hightempmetals.com/techdata/hitempKovardata.php> (accessed Jun. 15, 2023).
- [67] “Gold - Physical, Mechanical, Thermal, and Electrical Properties.” <https://www.azom.com/article.aspx?ArticleID=5147> (accessed Jul. 01, 2023).
- [68] N. He *et al.*, “Pyrolytic-carbon coating in carbon nanotube foams for better performance in supercapacitors,” *J. Power Sources*, vol. 343, pp. 492–501, Mar. 2017, doi: 10.1016/J.JPOWSOUR.2017.01.091.
- [69] M. S. Lal and S. Ramaprabhu, “High Areal Capacitance of Flexible Supercapacitors Fabricated with Carbon Cloth-Carbon Fiber-TiO₂ Electrodes and Different Hydrogel Polymer Electrolytes,” *J. Electrochem. Soc.*, vol. 169, no. 2, p. 020514, Feb. 2022, doi: 10.1149/1945-7111/AC4D6A.
- [70] W. Le Ma *et al.*, “An Overview of Stretchable Supercapacitors Based on Carbon Nanotube and Graphene,” *Chinese J. Polym. Sci. (English Ed.)*, vol. 38, no. 5, pp. 491–505, May 2020, doi: 10.1007/S10118-020-2386-X/METRICS.
- [71] Z. Zhai *et al.*, “A review of carbon materials for supercapacitors,” *Mater. Des.*, vol. 221, p. 111017, Sep. 2022, doi: 10.1016/J.MATDES.2022.111017.

List of Figures

Figure 2-1: Classification of different types of EDLCs and electrode materials used (redrawn from [7]).....	14
Figure 2-2: Energy-power density represented by Ragone plot for different energy storage systems (adopted and modified from [8].....	15
Figure 2-3: Schematic of EDLC showing its components [9]	16
Figure 2-4: Effects of different electrolyte on SC performance [adopted from [9].....	17
Figure 2-6: Carbon electrodes on Al foil (current collector) and separator used in EDLC [15].....	19
Figure 2-7: Schematic of charge and discharging mechanism in EDLC [18].....	20
Figure 2-8: Schematic of a PC showing its components [9].....	22
Figure 2-9: Diagram of SWCNT and MWCNT formed by rolling graphene sheets [11]	22
Figure 2-9: Illustration of chemically interconnected cross-linked CNT [22].....	23
Figure 2-11: Schematic of coin cell parts and configuration [42].....	26
Figure 2-12: Schematic of a pouch cell configuration [41].....	28
Figure 2-13: Chip-type EDLC from Seiko Instruments Inc. [40]	29
Figure 2-14: Major factors, metrics and test methods that are used for performance evaluation of SCs [46].....	30
Figure 2-15: SEM images of interconnected and cross-linked fullerene-like carbon decorated CNT (FC-CNTs) [22].....	32
Figure 2-16: Three-electrode system showing WE, RE and CE [45]	33
Figure 2-17: Schematic of (a-c) CV and (d-f) GCD curves for EDLC, PC and faradaic materials [48]	34
Figure 2-17: Schematic of a) Nyquist Impedance and b) Bode plot [7].....	35
Figure 2-18: A simplified representation of a Randles circuit to depict EIS [49]	36
Figure 3-1: Flowchart of the experimental setup and procedure for this study	37
Figure 3-2: Typical samples before and after the growth of CNTs.....	38
Figure 3-3: Glass fibre separator used in this study [14].....	40
Figure 3-4: Images of coin cell parts before and after packaging.....	42
Figure 3-5: Pouch cell packaging steps.....	42
Figure 3-6: Pouch cell configuration showing the components and sealing positions.....	43

Figure 3-7: Assembly setup for three-electrode system	44
Figure 3-8: Test setup for a) coin cell and b) pouch cell.....	45
Figure 4-1: FE-SEM images of CNTs with different Ni loading type, a) with Ni sputtering; b) NiSO ₄ solution dip coated; c) NiSO ₄ spray coated and d) NiSO ₄ drop coated	49
Figure 4-2: SEM cross-section of a Al-CNT sputtered sample showing thickness of the electrode	50
Figure 4-3: FTIR spectra of CNTs with different Ni loading, a) with sputtering; b) NiSO ₄ dip coated; c) NiSO ₄ spray coated and d) NiSO ₄ drop coated	51
Figure 4-4: a) Three-electrode and b) coin cell measurement for four different Al-CNT samples	53
Figure 4-5: Bar chart showing influence of mass loading & type of CNT sample on areal capacitance	54
Figure 4-6: CV curves for three-electrode measurement for CNT-SP2	56
Figure 4-7: Three-electrode measurement a) CV curves; and b) effect of scan rate on capacitance for CNT-SP3	56
Figure 4-8: CV curves for pouch and coin cell at scan rates a) 100 mV/s ; and b) 10 mV/s	57
Figure 4-9: Galvanostatic charge-discharge plot for pouch cell at 60 °C for different current densities	58
Figure 4-10: Areal capacitance and ESR at different temperature and cell configuration .	59
Figure 4-11: Bar chart showing the effect of coin cell crimp pressure on capacitance & ESR.....	62
Figure 4-12: Nyquist impedance plot at different crimp pressure	63
Figure 4-13: Bar chart showing the energy and power density at different crimp pressure	64
Figure 4-14: Graphs showing a) the cyclic stability and b) vaaariation from 1st and 2000th cycle for CNT-SP2 coin cell	65
Figure 4-15: Cross-sectional schematic of the proposed chip type SC.....	66
Figure 4-16: Detailed 3-D diagram and overview of the proposed chip type SC.....	67
Figure 4-17: Schematic of laboratory version of chip type SC.....	69
Figure 4-18: Attempted lab scale version of chip type SC with) Au deposited on Si wafer and b) partly etched Si wafer for prototype.....	70
Figure 4-19: CV curve for CNT-SP3 coin cell at different scan rates.....	72

Figure 4-20: Electrochemical impedance spectroscopy for CNT-SP3 coin cell showing a) Nyquist impedance plot; b) representation of Randle equivalent circuit with parameters; and c) circuit parameters found from fitting analysis73

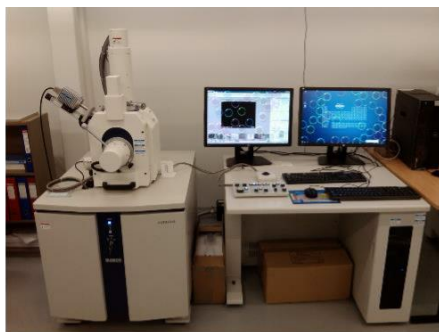
List of Tables

Table 2: Data for different CNT sample showing capacitance and mass loading	54
Table 3: Comparison of pouch cell and coin cell in terms of capacitance, energy density, power density, ESR and time constant.....	60
Table 4: Effect of coin cell crimp pressure on capacitance, power density, energy density and ESR.....	63
Table 6: Calculated parameters for the high performance CNT-SP3 coin cell.....	73
Table 7: Comparison of supercapacitor performance data from literature	74

Annexes

Equipment and Tools:

SEM



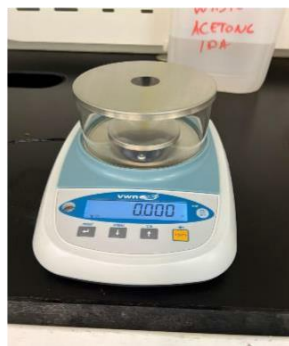
FESEM



FTIR



Scale



Ultrasonic Welding Machine



Ar filled-Glovebox



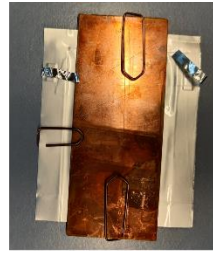
Heat Sealing Machine



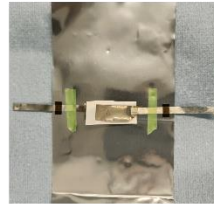
Vacuum-Heat Sealing Machine



Coin Cell Electrode Sizing & Preparation

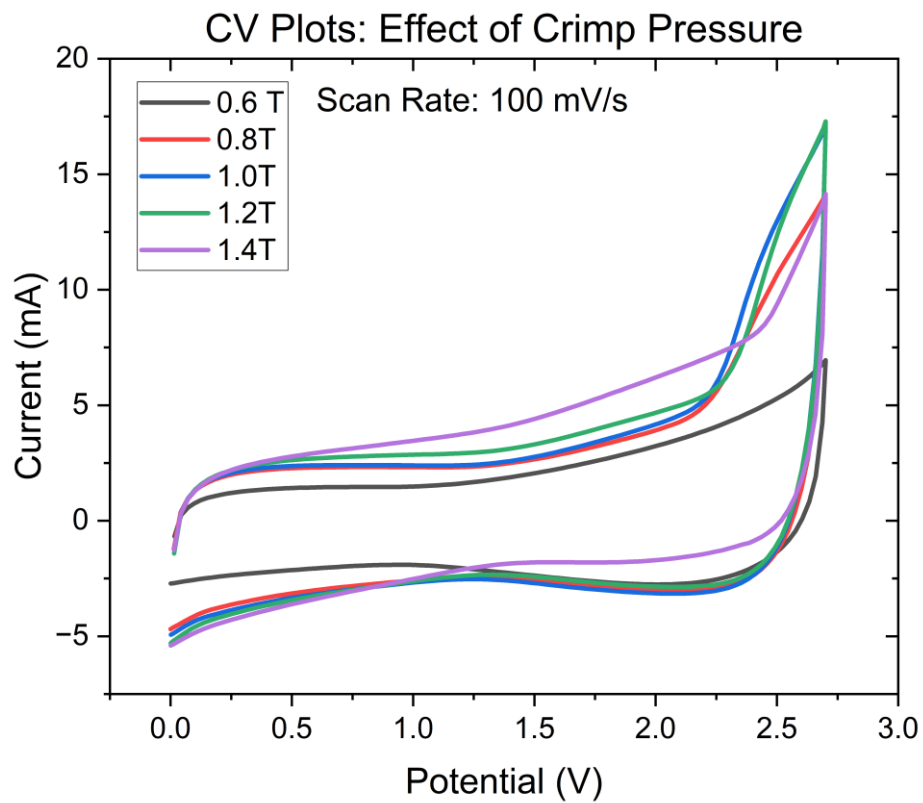


Pouch Cells Before & After Assembly

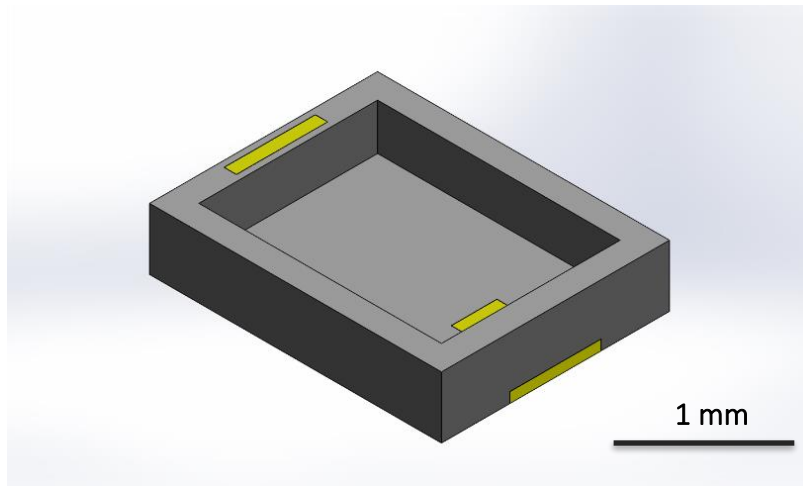


Potentiostat with climate chamber

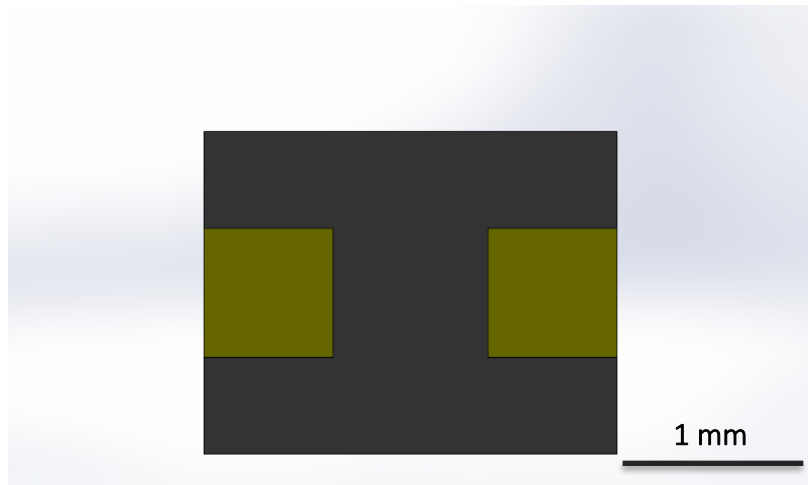
Effect of Crimp Pressure:



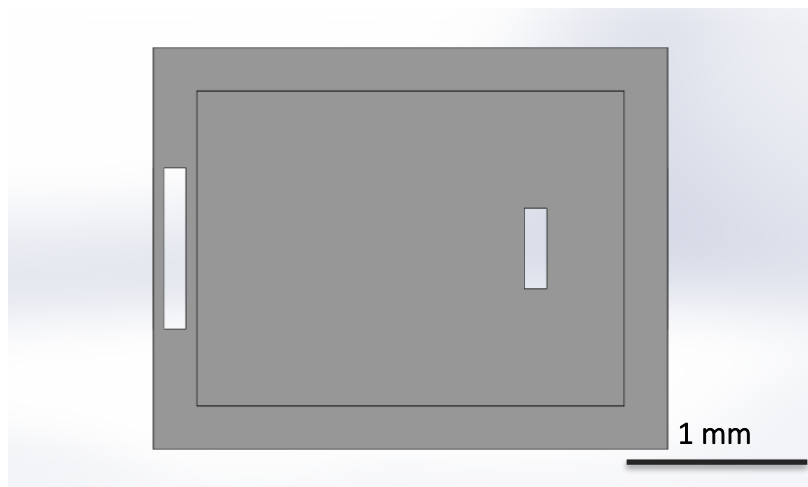
Chip Type Supercapacitor Proposed Design:



Ceramic Package Isometric View

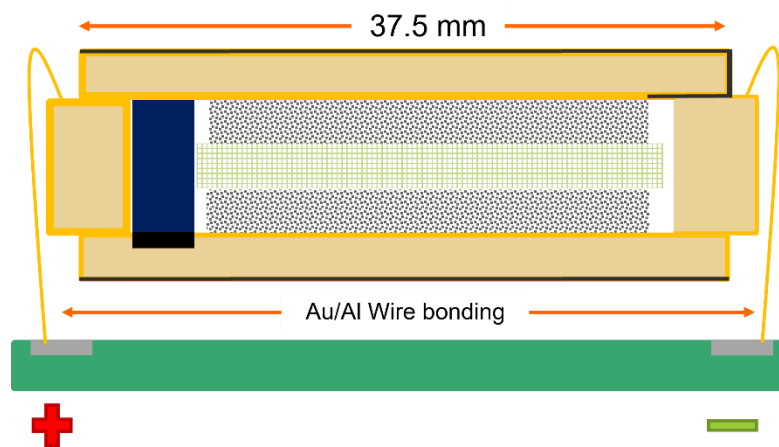







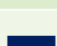

Ceramic Package Bottom View



Ceramic Package Top View

Chip Type SC: Lab Scale Version 2



	Description	Material Name
	Anode	CNT electrode
	Cathode	CNT electrode
	Conductor	Au
	Separator	Glass fiber
	Substrate	PCB
	Insulator	Non-conductive epoxy/SU8/PDMS
	Pad	Solder